U.S. DEPARTMENT OF THE INTERIOR
U.S. GEOLOGICAL SURVEY

TO ACCOMPANY MAP I–2677

GEOLOGIC MAP OF THE NULATO QUADRANGLE, WEST-CENTRAL ALASKA

By W.W. Patton, Jr. and E.J. Moll-Stalcup

DESCRIPTION OF MAP UNITS

OVERLAP ASSEMBLAGES

Surficial deposits

Qfy **Younger flood-plain deposits (Holocene)**—Chiefly light-gray micaceous silt along Yukon and Koyukuk Rivers. Silt, sand, and gravel along streams that drain bedrock uplands. Locally include some terrace and fan deposits along narrow tributary valleys. Characterized physiographically by bars, oxbow lakes, meander scrolls, abandoned channels, and other evidence of recent flood-plain building. Mapped almost entirely from aerial photographs.

Qfo **Older flood-plain deposits (Holocene or Pleistocene)**—Chiefly light-gray and grayish-orange micaceous silt. Subordinate lenses of sand and peat, reworked eolian sand, and gravel. Deposits are at or near river level but youthful flood-plain features such as oxbow lakes, meander scrolls, and abandoned channels are much modified or absent. Contact with younger flood-plain deposits (Qfy) locally gradational and poorly defined. Mapped almost entirely from aerial photographs.

Qhs **High-terrace and slope deposits (Pleistocene)**—Light-gray and grayish-orange micaceous silt deposits. Subordinate lenses of sand and peat. Deposits form a broad terrace 10 to 100 m above the floodplain of the Koyukuk Flats and extend as much as 250 m up the slopes of the bedrock hills surrounding the Flats. Terrace deposits characterized by thermokarst topography marked by many small lakes. Unit also forms terrace and slope deposits along streams that drain bedrock uplands and locally include coarse-grained colluvial and fan deposits.

Volcanic and intrusive rocks

Ta **Andesite and basalt (Eocene)**—Form a large area of columnar-jointed flows overlying marine and nonmarine deltaic deposits (Ks) of the Yukon-Koyukuk basin in the southwestern corner of the Nulato quadrangle and small flows overlying rocks of the basalt, gabbro, and chert unit (TrMb) and the quartzite, phyllite, and limestone unit (TrMq) of the Angayucham-Tozitna terrane in the southeastern corner of the Nulato quadrangle. Basalt is much less common than andesite and is distinguished solely on the basis of chemical composition. In southwest corner of the quadrangle andesite and basalt flows are composed of 5 to 10 percent phenocrysts of plagioclase, clinopyroxene, and less commonly orthopyroxene set in a groundmass of plagioclase microlites, granules of orthopyroxene, and opaque oxides. Some flows contain abundant dark, partly devitrified glass subophitically enclosing phenocrysts. Textures typical of calc-alkalic rocks and indicative of magma mixing are common, including glomeroporphyritic clots and strongly zoned and resorbed plagioclase phenocrysts. One andesite flow (81Pa321, table 4) contains a disequilibrium assemblage of quartz and strongly zoned plagioclase phenocrysts in a groundmass of granular clinopyroxene, opaque oxides, plagioclase microlites, and interstitial glass. Unit locally includes tuffs, breccias, and agglomerates in subordinate amounts. The basalt and andesite flows appear to underlie or are intruded by the rhyolite and dacite unit (Tr). The circular drainage pattern of Poison Creek in the Nulato quadrangle and Stink Creek in the adjoining Norton Bay quadrangle

appears to outline a volcanic depression or "caldera" about 12 km in diameter within the area covered by these flows. In the southeastern part of the quadrangle the unit is represented by two small columnar jointed andesite porphyry flows composed of 5 to 7 percent phenocrysts of ortho- and clinopyroxene and plagioclase set in a groundmass of plagioclase microlites, granular orthopyroxene, opaque oxides, and dark partially devitrified glass.

The basalt and andesite unit is assigned an Eocene age on the basis of three whole rock K-Ar ages ranging from 52.4±1.6 to 56.5±1.7 Ma from exposures on the west bank of the Yukon River (no. 1, table 1 and fig. 22).

Tr **Rhyolite and dacite (Eocene)**—Unit overlies and intrudes nonmarine and marine deltaic deposits (Ks) of the Yukon-Koyukuk basin in the southwest corner of the Nulato quadrangle. East of the Yukon River in the south-central and southeastern part of the quadrangle it forms small sparsely distributed bodies that overlie and intrude the schist and quartzite unit (P_zPs) of the Ruby terrane and the basalt, gabbro, and chert unit (T_rMb) of the Angayucham-Tozitna terrane. The rhyolite and dacite unit is spatially associated with the andesite and basalt map unit (Ta) and forms a compositionally continuous suite with that unit. The rhyolite and dacite unit is composed of finely banded flows, tuffs, breccias, and hypabyssal domal intrusive bodies. The rhyolite consists of 2 to 5 percent fine-grained phenocrysts of plagioclase, biotite, magnetite, and, in places, quartz and anorthoclase in a groundmass of devitrified glass. The dacite consists of 2 to 25 percent phenocrysts of oligoclase, magnetite, and either granular pyroxene or green hornblende and biotite in a groundmass of plagioclase microlites and glass. Spherulitic growths, including some lithophysae, are common. The degree of devitrification varies: some samples have retained abundant glass and display a vitrophyric texture; others are composed almost entirely of aphyric perlitic glass. The hypabyssal domal intrusive bodies are composed of phenocrysts of plagioclase, biotite, and hornblende in a finer crystalline groundmass of plagioclase, quartz, and potassium feldspar(?). The domal intrusive bodies typically are deeply weathered and in several places form prominent reddish-orange limonite gossans. Three samples of the rhyolite and dacite unit were analyzed chemically: two from the southwest corner of the quadrangle (81Pa319 and 82Pa76, table 3) and one from the southeast part of the quadrangle (79Pa519, table 3).

The rhyolite and dacite unit is assigned an Eocene age on the basis of two K-Ar mineral-separate ages obtained from dacite exposures along the west bank of the Yukon River (table 1; fig. 22). Sample 81APa319 (no. 3) yielded ages of 50.6±1.5 (biotite) and 47.6±1.4 (hornblende) Ma and sample DT 83-15A (no. 2) yielded ages of 53.3±1.6 (biotite) and 49.1±1.5 (hornblende) Ma.

TKi **Shallow intrusive rocks of silicic and intermediate composition (early Tertiary and Late Cretaceous)**—Includes a wide variety of shallow intrusive rocks including rhyolite, dacite, and andesite plugs, domes, sills, and dikes and larger more coarsely crystalline bodies of granite, granodiorite, tonalite, and monzonite porphyry. Unit is confined to the northeastern part of the quadrangle where it intrudes sedimentary deposits of the Yukon-Koyukuk basin (map units Ks, Kg) and andesitic volcanic rocks (map unit Kv) of the Koyukuk terrane. The unit is poorly exposed and has not been studied in detail. Thin-section examination was limited to four samples from widely separated localities. The coarser grained bodies typically have a porphyritic texture consisting of phenocrysts of feldspar and biotite or hornblende set in a finer crystalline groundmass of feldspar, quartz, and subordinate mafic minerals. A thin section from a columnar-jointed plug-like dacite body forming Meuller Mountain, 25 km east of Galena, consists of 7 percent phenocrysts of strongly zoned plagioclase and a greenish-brown alteration mineral, probably replacing amphibole, in a fine-grained groundmass of plagioclase laths and minor interstitial quartz.

The unit is provisionally assigned an early Tertiary and Late Cretaceous age. No isotopic age data are available for these rocks in the Nulato quadrangle, but to the northeast, in the adjoining Melozitna quadrangle, similar intrusive rocks yield a Late Cretaceous isotopic age (Patton and others, 1978) and to the southwest, in the adjoining Unalakleet quadrangle, a similar assemblage of shallow intrusive rocks yield early Tertiary and latest Cretaceous isotopic ages (Patton and Moll-Stalcup, 1996).

Complex of small intrusive bodies and thermally altered sedimentary deposits

TKis **Shallow intrusive rocks of silicic and intermediate composition (early Tertiary and Late Cretaceous), marine and nonmarine sandstone, shale, and conglomerate deltaic deposits (Late and Early Cretaceous), and volcaniclastic graywacke and mudstone turbidite deposits (Early Cretaceous), undivided**—Small bodies of rhyolite, dacite, and andesite porphyry and larger more coarsely crystalline bodies of granite, granodiorite, tonalite, and monzonite porphyry intruding thermally altered sedimentary deposits of the Yukon-Koyukuk basin. The intrusive bodies are too small and too numerous to be mapped separately at this map scale. Sedimentary host rocks are altered to an erosion-resistant hornfels. The complex forms a broad domal topographic feature and prominent landmark in the northeastern part of the Nulato quadrangle and in the adjoining Ruby quadrangle. The complex is interpreted to represent the roof of a shallow pluton (map sheet, section *B–B′*). Similar complexes have been reported to the southwest in the Unalakleet quadrangle (Patton and Moll-Stalcup, 1996).

Yukon-Koyukuk basin sedimentary deposits

Ks **Nonmarine and marine sandstone, shale, and conglomerate deltaic deposits, undivided (Late and Early Cretaceous)**—Well-sorted, medium- to coarse-grained, light-olive crossbedded sandstone, fine- to medium-grained, dark-gray to green silty sandstone, dark-gray micaceous shale, quartz-chert-pebble conglomerate, and thin seams of bituminous coal. The unit is composed of nonmarine, fluvial, delta-plain deposits that grade downward into marine delta-front deposits. It appears to have had its source to the east and to fine westward; paleocurrent directions are westward (Nilsen, 1989). The total thickness of the unit along the west bank of the Yukon River between the mouth of the Koyukuk River and the Kaltag Fault is estimated to be 750 m (Patton and Bickel, 1956). Along the western boundary of the Nulato quadrangle the thickness of the unit is estimated to be 2,500 m (Bickel and Patton, 1957).

The nonmarine fluvial deposits are characterized by fine-grained, locally cross-bedded quartzose sandstone that characteristically weathers to a rusty yellow orange. The sandstone is interbedded with dark-grayish-olive to gray micaceous shale and siltstone. Near the base, the fluvial beds are composed of fine- to coarse-grained, lenticular, cross-bedded, friable sandstone and conglomerate containing pebble- to grit-size clasts of quartz and chert with lesser amounts of mafic intrusive and extrusive rocks, and schist. Bituminous coal seams have been reported in the nonmarine strata at several localities along the west bank of the Yukon River near the village of Nulato (Wahrhaftig and others, 1994; Barnes, 1967). They were mined in the early days of the goldrushes to the Klondike and to other parts of Alaska, chiefly for river steamboat fuel. The mine sites have long since disappeared and the seams are now largely covered with talus. The reported mine sites include a 50- to 100-cm-thick seam 15 km north of Nulato, a 15-cm-thick seam 1.5 km north of Nulato, a seam less than 60 cm thick 6 km south of Nulato, and sheared pockets of coal as much as 2.5 m across 15 km south of Nulato. The nonmarine beds contain abundant fresh- and brackish-water mollusks and well-preserved plant remains of Late Cretaceous (Cenomanian and Turonian?) age (R.A. Spicer, oral communication, 1987). For the location of plant fossil and mollusk collections from these beds

on the Yukon River the reader is referred to Patton and Bickel (1956).

Ksm **Marine deltaic deposits (Late and Early Cretaceous)**—The marine deposits in the lower part of the unit are mapped separately along the Yukon River below the mouth of the Koyukuk River and in the drainage basins of the Nulato River and the Gisasa River in the northwestern corner of the quadrangle. These deposits represent a marine tongue that underlies the fluvial deposits and thickens westward. On the Yukon River the marine deposits have an estimated thickness of 425 m and consist of pale-olive to gray, fine- to coarse-grained, crossbedded, lenticular sandstone grading down into dark-greenish-gray, fine-grained sandstone and interbedded dark-gray siltstone and shale (Patton and Bickel, 1956). In the Nulato River and Gisasa River drainages the marine deposits are composed predominantly of siltstone and shale and have an estimated thickness of about 1300 m (Bickel and Patton, 1957). The marine deposits are assigned an Early Cretaceous (middle Albian) age on the basis of an abundant molluscan fauna including *Inoceramus altifluminis* McLearn, *Yaadia whiteavesi* (Packard), *Gastroplites* sp., and *Paragastroplites flexicostatus* Imlay (Elder and Miller, 1991). Extensive fossil collections have been made from this unit by several workers along the Yukon River and in the Nulato River and Gisasa River drainages. The locations of the most significant collections are shown on fig. 23 and listed in table 2. Additional collections from this unit have been reported by Patton (1966) a short distance north of the Nulato quadrangle in the adjoining Kateel River quadrangle.

Kcs **Calcareous sandstone, siltstone, and shale turbidite deposits (Early Cretaceous)**—Fine- to coarse-grained, dark-greenish-gray, moderately to highly calcareous, turbiditic sandstone interbedded with dark-gray shale and siltstone. The sandstone occurs in beds 0.5 to 1 m thick grading upward into finely cross-laminated, muscovite-rich siltstone and shale. The base of sandstone beds commonly is marked by flute casts, ripple marks and rip-up clasts of underlying shale layers along with quartz and chert grit. The siltstone and fine-grained sandstone generally contain thin layers of finely comminuted, carbonized plant debris. Calcareous discoidal concretions as much as 20 cm in diameter are common. The sandstone typically consists of poorly sorted clasts of quartz, chert, feldspar (chiefly plagioclase), muscovite, and carbonate rocks in a carbonate-rich matrix. Carbonate composes as much as 50 percent of the sandstone. This unit crops out in a 15-kilometer-wide belt in the northwestern part of the Nulato quadrangle, bordered on the northwest by the volcaniclastic graywacke and mudstone turbidite map unit (Kg) and on the southeast by the marine deltaic map unit (Ksm). Typically this unit forms smooth rounded uplands in contrast to the more angular crests and steeper slopes that characterize adjoining map units Kg and Ksm. The contacts with these bordering units appear to be high-angle faults. The best exposures are along the Gisasa River where many of the beds are overturned. The turbidite deposits that characterize this unit are interpreted as a prodelta facies correlative in age with the marine sandstone, siltstone, and shale deltaic deposits of map unit Ksm. The unit is assigned an Early Cretaceous (middle Albian) age based on the occurrence of the ammonite *Gastroplites* sp. on the southwesterly extension of this unit in the adjoining Norton Bay quadrangle (Elder and Miller, 1991).

Kg **Volcaniclastic graywacke and mudstone turbidite deposits (Early Cretaceous)**—Dark-gray to green, hard, fine-grained to conglomeratic, volcanic graywacke and dark-gray finely laminated mudstone. The graywacke is composed of matrix-supported intermediate and mafic volcanic and intrusive rock and chert clasts; quartz and metamorphic rock clasts are present in subordinate amounts. Some of the graywacke beds are characterized by a distinctly mottled appearance owing to the presence of laumontite (Hoare and others, 1964). The base of the unit is marked by a pebble-granule conglomerate composed almost entirely of mafic volcanic and

intrusive clasts. In the upper part of the unit metamorphic detritus becomes increasingly abundant. The depositional environment of this unit is uncertain owing to the absence of good exposures; presumably it represents a transition from shelf to basin environment. The unit crops out in two small areas within the Nulato quadrangle: (1) north of the Yukon River in the northeastern corner of the quadrangle and (2) in a tiny area between Arvesta Creek and the extreme northwest corner of the quadrangle. Exposures in these areas are limited to small patches of frost-riven rubble. The unit is overlain by nonmarine and marine deltaic deposits of the Yukon Koyukuk basin (map unit Ks) and, in the northeastern part of the quadrangle, unconformably underlain by the andesitic volcanic and volcaniclastic rocks of the Koyukuk terrane (map unit Kv). The unit appears to be transitional in composition between the poorly sorted volcaniclastic rocks of Kv and the better sorted deltaic deposits of Ks.

No fossils have been found in this unit in the Nulato quadrangle. However, the ammonite *Paragastroplites* sp. of Early Cretaceous (middle Albian) age was identified in this unit in the adjoining Kateel River quadrangle 15 km north of the boundary of the Nulato quadrangle (Elder and Miller, 1991). Similar volcaniclastic graywacke and mudstone turbidite deposits elsewhere in the Yukon-Koyukuk basin have yielded fossils of Early Cretaceous (Aptian(?) to middle Albian) age (Box and others, 1985).

Khotol pluton

Kgr **Granite (Early Cretaceous)**—This unit is confined to the Khotol pluton, a large granite body 12 by 20 km in size in the Kaiyuh Mountains in the south-central part of the Nulato quadrangle. Exposures of the Khotol pluton are limited to a few small outcrops and to scattered large blocks of rubble. The granite typically is coarsely porphyritic and consists of large K-feldspar phenocrysts set in a moderately coarse allotriomorphic groundmass of K-feldspar, plagioclase, quartz, biotite, apatite, zircon, and sphene. Grain boundaries are commonly granulated and biotite grains are slightly deformed. Some quartz grains show undulatory extinction. Locally the plagioclase is partly altered to sericite and the biotite partly altered to chlorite. The granite intrudes the schist and quartzite map unit (PzPs) of the Ruby terrane, which is thermally altered near the perimeter of the pluton to an andalusite-bearing hornfels. The granite displays gneissic banding locally along the margins of the pluton.

The Khotol pluton is assigned an Early Cretaceous age on the basis of a single K-Ar cooling age of 112±3.4 Ma (no. 4, table 1 and fig. 22) from a biotite mineral separate. The pluton is interpreted to represent the southern lobe of the Melozitna pluton that has been offset right-laterally by the Kaltag Fault about 130 km to its present position (Patton and others, 1984). The Melozitna pluton is located on the north side of the Kaltag Fault in the Melozitna quadrangle northeast of the Nulato quadrangle.

LITHOTECTONIC TERRANES

Koyukuk terrane

The Koyukuk terrane of west-central Alaska underlies a large part of the Yukon-Koyukuk basin and has been described in detail by Box and Patton (1989) and Patton and others (1994) as a volcanic arc terrane. In the Nulato quadrangle the Koyukuk terrane is composed of andesitic volcanic rocks (Kv) of Early Cretaceous age and ultramafic-mafic complexes (Juu, Jcu, Jht) of Late and Middle Jurassic age.

Kv **Andesitic volcanic rocks (Early Cretaceous)**—Andesite and basalt flows, volcaniclastic rocks, and subordinate rhyolite and dacite flows. The andesite and basalt flows typically are porphyritic with phenocrysts of plagioclase set in a matrix of devitrified glass, altered plagioclase microlites, pyroxene, chlorite, and opaque oxides. Vesicles are commonly filled with calcite. The volcaniclastic rocks range in clast size from coarse breccia and conglomerate to lapilli and fine cherty tuff. The clasts consist of dark-red to green, angular to subrounded fragments of andesite and basalt flows, cherty tuff, and crystals

of plagioclase, clinopyroxene, and hornblende in a matrix of devitrified glass. Typically there is an upward grading from coarse breccia to lapilli tuff to fine-grained, blue-green cherty tuff. In the Nulato quadrangle outcrops of this map unit are confined to several small widely scattered localities in the northeastern and north-central part of the Nulato quadrangle and in the Magitchlie Range in the southwestern part of the quadrangle. The best exposures occur in massive cliffs along the Koyukuk River, a short distance north of the village of Koyukuk. Scattered rubble outcrops of this unit form low hills on the east side of the Koyukuk Flats north of the Yukon River and underlie Pilot Mountain, a prominent landmark in the central part of the Flats, 20 km west of the village of Galena. Aeromagnetic data (Zietz and others, 1959) suggest that large parts of the Koyukuk Flats are underlain by this unit. In the Magitchlie Range, at the south edge of the Flats, the unit is exposed in narrow slivers that are in fault contact with the basalt, gabbro, and chert unit (TrMb) of the Angayucham-Tozitna terrane and are overlapped by nonmarine conglomerate and sandstone deltaic deposits of map unit Ks.

Two collections (nos. 27 and 28, table 2 and fig. 23) of the fossil mollusk *Buchia* from volcaniclastic rocks provide an Early Cretaceous (Valanginian) age for this map unit and support correlation with similar volcanic assemblages in the Koyukuk terrane elsewhere in the Yukon-Koyukuk basin. *Buchia sublaevis* (Pavlow) was collected in the vicinity of Pilot Mountain in the central part of the Koyukuk Flats and *Buchia crassicolis solida* (Lahusen) was found on the east side of the Flats in the northeastern part of the quadrangle (table 2). Harris and others (1987) obtained K-Ar ages of 108.1±3.2, 111.9±3.4, and 113.2±3.4 Ma for plagioclase mineral separates from andesite and basalt flows that crop out near the mouth of the Koyukuk River. These ages are younger than any of the K-Ar or fossil ages obtained from other volcanic rock exposures of Koyukuk terrane in the Yukon-Koyukuk basin (see, for example, Box and Patton, 1989) and suggest that they may have been reset by a younger thermal event.

Juu **Ultramafic-mafic complexes, undivided (Late and Middle Jurassic)**—Composed of partially serpentinized peridotite and dunite intruded by narrow dikes of fresh clinopyroxenite, hornblendite, gabbro, and gabbro pegmatite. At several localities the bases of the complexes are marked by finely layered, highly tectonized amphibolite, garnet amphibolite, and pyroxene granulite. The gabbro and gabbro pegmatite are fine- to medium-grained hypidiomorphic rocks composed of plagioclase laths, euhedral brown to green amphibole and accessory sphene, apatite, epidote, and opaque oxides. The amphibolite and granulite at the base of the complexes also contain abundant plagioclase and amphibole but have a nematoblastic texture and locally contains up to 15 percent garnet and/or clinopyroxene. Eight chemical analyses for samples of the gabbro, gabbro pegmatite, and amphibolite are given in table 9. The ninth analysis is for a sample of diorite (82Pa4) from the Magitchlie Range, which is provisionally assigned to this map unit, but is of uncertain affinities.

The ultramafic-mafic complexes crop out along the Yuki River in the southeastern part of the Nulato quadrangle and in two small areas near the southern border of the quadrangle in the Little Mud River drainage. All of the complexes along the Yuki River appear to be klippen resting in thrust fault contact on rocks of the Angayucham-Tozitna terrane. The small complexes in the Little Mud River drainage are surrounded by surficial deposits and their relationship to the underlying bedrock is uncertain. The largest and best-studied complex is located in the upper Yuki River drainage where it forms a prominent mountain, 685 m in elevation. Loney and Himmelberg (1984) studied this complex in detail and recognized two subunits, which are shown on the map sheet as Jcu and Jht.

Jcu **Cumulate ultramafic rocks**—Consists predominantly of dunite, but also includes bodies of wehrlite and olivine

clinopyroxenite that range in thickness from a few meters to a few tens of meters. Some harzburgite occurs locally in the unit but is interpreted to be part of the harzburgite tectonite unit infolded into the cumulate sequence. Two exposures of massive chromitite as much as 1.5 m thick were noted in dunite cumulate. Elsewhere chromite is restricted to centimeter-scale layers in dunite and as an accessory mineral.

Jht **Harzburgite tectonite**—Consists of harzburgite composed of 20–30 percent orthopyroxene, as much as 75 percent olivine, and minor amounts of clinopyroxene and spinel. The harzburgite is partly serpentinized, but its primary mineralogy and structure are easily distinguishable. Dunite occurs locally in the harzburgite as centimeter-scale layers and as lenses as much as several tens of meters thick. Harzburgite is well-foliated to massive. Foliation results from gradational variations in the ratio of olivine to orthopyroxene.

The ultramafic-mafic complexes in the Nulato quadrangle were previously regarded as belonging to an upper thrust panel of the Angayucham-Tozitna oceanic terrane (Patton and Box, 1989). However, more recent studies suggest that they are part of the Koyukuk volcanic-arc terrane (Patton, 1993; Patton and Moll-Stalcup, 1996).

The ultramafic-mafic complexes are assigned a Late and Middle Jurassic age on the basis of: (1) correlations with similar complexes located on the Ruby geanticline northeast of the Nulato quadrangle (Patton, 1992) and (2) a single Late Jurassic K-Ar amphibole age of 151±4.5 Ma obtained from a gabbro pegmatite dike that cuts one of the small complexes in the Little Mud River drainage (no. 5, table 1 and fig. 22). An anomalous age of 269±8 Ma was measured on a hornblende pegmatite from a tiny complex in the Yuki River drainage (no. 7, table 1 and fig. 22). This age cannot be reconciled with previously reported K-Ar ages from any of the ultramafic-mafic complexes elsewhere on the Ruby geanticline. A Middle Jurassic K-Ar age of 172±5.2 Ma was measured on metamorphic amphibole from amphibolite at the base of the largest complex in the Yuki River drainage (no. 6, table 1 and fig. 22). Similar metamorphic mineral ages have been obtained from the base of ultramafic-mafic complexes elsewhere on the Ruby geanticline (Patton, 1992).

Angayucham-Tozitna terrane

The Angayucham-Tozitna terrane occupies a broad area in the southeastern and south-central parts of the Nulato quadrangle between the Yukon River and the southern boundary of the quadrangle. It also crops out in the Magitchlie Range in the southwestern part of the quadrangle. An altered basalt, gabbro, and chert unit (TrMb) makes up the bulk of the terrane and is typical throughout the region. A second unit of quartzite, phyllite, and limestone (TrMq) is questionably assigned to this terrane and is confined to two large klippen and to a poorly exposed fault-bounded(?) belt.

TrMb **Altered basalt, gabbro, and chert (Triassic to Mississippian)**—Variably altered and metamorphosed dark-green to gray flows and shallow intrusives of basalt, diabase, and gabbro locally interlayered with volcaniclastic rocks of basaltic composition, bedded chert, and argillaceous rocks. Unit is best exposed in the Kaiyuh Mountains where it lies in apparent thrust fault contact on the schist and quartzite map unit (PzPs) of the Ruby terrane (map sheet, section *C–C'*). Southeast of the Kaiyuh Mountains exposures are confined to scattered rubble crops on the crest of low hills and to a few isolated cutbanks along the small drainages. Sill-like bodies of gabbro and diabase underlie many of the higher elevations and cap prominent flat-topped or gently dipping mesas and buttes along the boundary with the Ruby terrane in the Kaiyuh Mountains. In the Kaiyuh Mountains near the thrust contact with the Ruby terrane the unit is strongly foliated, ductily deformed, and contains high-pressure and low-temperature mineral assemblages characterized by actinolite, clinopyroxene, chlorite, plagioclase, epidote, and glaucophane, with or without lawsonite, stilpnomelane or pumpellyite, and with accessory sphene and magnetite. Plagioclase grains are saussuritized and albitized. According to Sarah Roeske

(written commun., 1995) the reaction textures are consistently zoned so that the relict clinopyroxene is mantled by actinolite, which in turn is mantled by glaucophane. This suggests that the actinolite may have formed during seafloor metamorphism and later was overprinted by subduction metamorphism. Southeast of the Kaiyuh Mountains in the Yuki River drainage basin the unit is only slightly foliated and in some places relict igneous textures and remnants of pillow structures are discernible. The unit in this part of the quadrangle is characterized by low-grade greenschist facies metamorphic assemblages typified by partly albitized and saussuritized plagioclase containing abundant clay minerals and clinopyroxene rimmed with actinolite, chlorite, calcite, and epidote. Prehnite and pumpellyite were identified in several samples. The abrupt transition across a relatively narrow covered zone from the high-pressure, low-temperature metamorphic assemblages in the Kaiyuh Mountains to the weakly metamorphosed assemblages that lie to the east suggests that the two different metamorphic facies may have been juxtaposed by an unrecognized low-angle thrust fault.

Volcanic breccia, conglomerate, and crystal and lithic tuffs occur in subordinate amounts interlayered with the basalt and gabbro flows and sills. These clastic rocks consist of angular to subrounded granule- to boulder-size fragments of basalt, diabase, cherty tuff, and chert set in a dark-green tuffaceous matrix. The mafic rock clasts and the matrix are compositionally similar to the altered basalt and gabbro that make up the bulk of this unit.

Green, gray, black, and red radiolarian bedded chert is abundant in this map unit in the Yuki River drainage area. Exposures are limited largely to rubble outcrops, but the few rare intact exposures show clearly that the chert is bedded and interlayered with the basalt flows and argillaceous rocks. Typically the chert consists of banded lighter and darker shades of gray and green, but black chert and reddish jasperoidal chert were noted in several places. All gradations from pure glassy translucent chert to impure cherty tuff to very fine grained tuff occur. Samples of the chert containing radiolarians were collected at four localities in the central part of the Angayucham-Tozitna belt in the Nulato quadrangle (nos. 29–32, table 2 and fig. 23). Three of these collections yielded Carboniferous ages and the fourth gave a Late Triassic age. A single radiolarian collection in the adjoining Ruby quadrangle, 2 km east of the border with the Nulato quadrangle, also yielded a Carboniferous age.

Argillaceous rocks are widely dispersed as finely divided rubble among outcrops and coarser rubble fragments of the more resistant basalt, gabbro, and chert of this unit. The argillaceous rocks vary in degree of induration and metamorphism from place to place and locally can be described as slate, argillite, or phyllite. Structural characteristics of the argillaceous rocks could not be determined from exposures. Because they are poorly exposed and less resistant to erosion than other rocks of this unit, it is not possible to estimate how much of the unit they comprise.

Angayucham-Tozitna terrane (?)

TrMq **Quartzite, phyllite, and limestone (Triassic? to Mississippian?)**—Interbedded white to light-gray banded quartzite, dark phyllite, and gray laminated limestone form two klippen overlying Ruby terrane in the Kaiyuh Mountains (section *C*–*C′*). Similar quartzite and phyllite also occur in a fault-bounded (?) band about 5 km wide along the poorly exposed contact of the Angayucham-Tozitna and Ruby terranes in the southeast corner of the Nulato quadrangle. No limestone was found along this band. Thin sections show the quartzite to be composed of as much as 99 percent interlocking quartz grains. Thin layers of white mica folia give the quartzite a faint foliation. Some samples from the two klippen overlying Ruby terrane contain a blue amphibole (riebeckite or crossite) and suggest that the unit underwent the same high-pressure low-temperature metamorphic event as the underlying Ruby terrane.

The white and light-gray banding and purity of the quartzites and the even texture of the quartz grains suggest that the quartzite maybe be a recrystallized chert (metachert), possibly a metamorphosed correlative of the bedded chert in map unit TrMb. The quartzite is locally interlayered with dark-gray, finely laminated, slightly foliated siliceous argillite, dark phyllite, and a talcy chloritic schist. In the Kaiyuh Mountains this map unit is exposed in small mesas structurally overlain by small remnants of a flat to gently dipping thrust sheet of gabbro presumedly belonging to map unit TrMb. The strata underlying the fault contact show strong evidence of ductile strain including deformed quartz veins and boudins and blocks of laminated limestone in deformed quartzite. The limestone is partly recrystallized and silicified and locally contains unidentifiable coral and crinoid fragments.

The quartzite, phyllite, and limestone unit is not widely exposed in the Nulato quadrangle and its stratigraphic relationship to adjoining map units in the Angayucham-Tozitna and Ruby terranes is poorly understood. In the Kaiyuh Mountains and in the southeastern part of the quadrangle the unit appears to occupy a structural position between the Ruby terrane and unit TrMb of the Angayucham-Tozitna terrane. All contacts with these adjoining units appear to be faults. The unit is tentatively assigned to the Angayucham-Tozitna terrane based on the interpretation that the quartzite is a metachert and correlative with chert in unit TrMb. It is possible, however, that this unit represents a separate lithotectonic terrane.

Ruby terrane

The Ruby terrane underlies the higher elevations of the Kaiyuh Mountains in a southwest-trending belt that stretches diagonally across the central part of the Nulato quadrangle from the Kaltag Fault to the south edge of the quadrangle. It also occurs in a narrow fault-bounded(?) southwest-trending belt in the southeast corner of the quadrangle. Most of the terrane consists of schist and quartzite (PzPs), but it also contains subordinate layers of carbonate rocks (Pzc) and metabasite (PzPm), which have been mapped separately where identified in the field. All of these rocks were subjected to high-pressure low-temperature metamorphism, as defined by the presence of glaucophane and lawsonite. Subsequently they were overprinted by low greenschist-facies metamorphism and thermally altered around the perimeter of the Khotol pluton.

Pzc **Carbonate rocks (Early Paleozoic)**—Gray to white, partly to wholly recrystallized limestone, dark-gray dolomite, and impure schistose limestone. Unit occurs in layers as much as 25 m thick intercalated with quartz-mica schist, mica schist, graphitic schist, metabasite, and quartzite. Some contacts are gradational; others are sharp and may be faulted. The unit is assigned an early Paleozoic age on the basis of early Middle Ordovician conodonts collected from carbonate rocks in the southern part of the Kaiyuh Mountains (A.G. Harris, written commun., 1984) (no. 33, table 2 and fig. 23) and Devonian corals collected from carbonate rocks in the adjoining Ruby quadrangle, about 10 km east of the Nulato quadrangle (Mertie and Harrington, 1924). Map shows only the larger bodies of these carbonate rocks where observed in the field or on aerial photographs. Undoubtedly many additional unrecognized bodies of carbonate rocks exist in areas mapped as unit PzPs.

PzPm **Metabasite (Paleozoic and Proterozoic?)**—Green to dark-greenish-gray, thinly layered greenschist and more massively layered greenstone. Greenstone bodies are schistose near contacts and only mildly foliated in the interiors. Unit appears to represent metamorphosed flows, tuffs, and shallow intrusive bodies of mafic and intermediate composition that were intercalated with the metasedimentary rocks of units PzPs and Pzc. Typical mineral assemblages are: (1) albite, chlorite, actinolite, and epidote group minerals, with or without calcite or sphene; and (2) glaucophane, chlorite, epidote, white mica, garnet, and quartz, with or without stilpnomelane(?) or chloritoid(?). Map shows only a few larger bodies of the metabasite where observed in the field. Numerous other bodies of metabasite may not have been recognized during field mapping or are

too small to be mapped separately, and are included in map unit PzPs.

PzPs **Schist and quartzite (Paleozoic and Proterozoic?)**—Consists chiefly of quartzite, quartz-mica schist, chlorite schist, and micaceous and graphitic quartzite. The unit also includes unknown thicknesses of poorly exposed fine-grained pelitic schist and phyllite. Typical mineral assemblages in the quartzite and quartz-mica schist are: (1) quartz, white mica, and chlorite, with or without chloritoid, clinozoisite, or plagioclase; and (2) quartz, white mica, glaucophane, garnet, chlorite, and chloritoid. Andalusite, biotite, and post-kinematic garnet occur in the contact aureole of Khotol pluton. A protolith age for at least part of this unit is early Paleozoic on the basis of the fossils recovered from interlayered carbonate rocks of unit Pzc (see above). However, isotopic studies by Arth and others (1989) of granitic plutons that intrude this unit elsewhere in the southern part of the Ruby terrane suggest that some of the unit may be as old as Proterozoic. Regional blueschist-greenschist metamorphism of the unit clearly pre-dated intrusion of the mid-Cretaceous Khotol pluton and probably occurred in latest Jurassic to Early Cretaceous time. Two samples collected from the Ruby terrane outside the thermal aureole of the Khotol pluton yield metamorphic muscovite K-Ar ages of 134±4.0 and 134±4.1 Ma (nos. 8 and 9, table 1 and fig. 22).

GEOLOGIC SETTING

INTRODUCTION

The Nulato quadrangle encompasses approximately 17,000 km^2 (6,500 mi^2) of west-central Alaska within the Yukon River drainage basin. The quadrangle straddles two major geologic features—the Yukon-Koyukuk sedimentary basin, a huge triangle-shaped Cretaceous depression that stretches across western Alaska from the Brooks Range to the Yukon delta; and the Ruby geanticline, a broad uplift of pre-Cretaceous rocks that borders the Yukon-Koyukuk basin on the southeast. The Kaltag Fault crosses the quadrangle diagonally from northeast to southwest and dextrally offsets all major geologic features as much as 130 km (fig. 1).

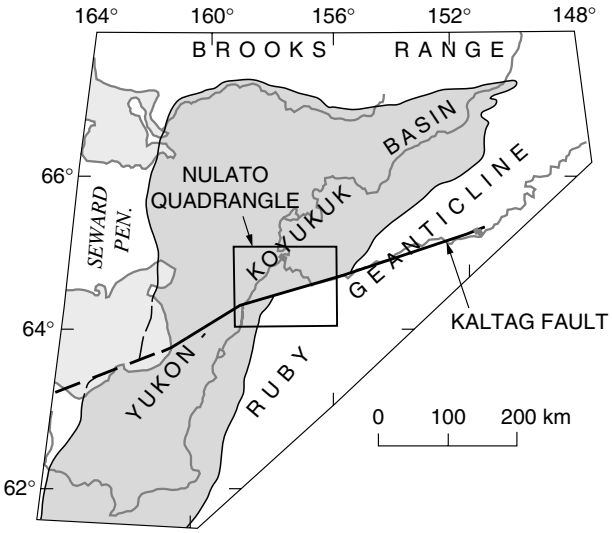

Figure 1. Map showing relationship of Nulato quadrangle to the major structural features of west-central Alaska.

YUKON-KOYUKUK BASIN

The Yukon-Koyukuk basin is filled with overlap assemblages composed of terrigenous sedimentary deposits that are distributed in two vaguely defined subbasins, the Lower Yukon and the Kobuk-Koyukuk (Patton and Box, 1989) (fig. 2). The Lower Yukon subbasin is confined to a triangular-shaped area in the northwestern part of the quadrangle between the Yukon River and the western border of the quadrangle. The Kobuk-Koyukuk subbasin occupies the northeastern corner of the quadrangle and a small area in the southwestern corner of the quadrangle south of the Kaltag Fault. It is dextrally offset 100 to 130 km by the Kaltag Fault. Sedimentary deposits in both subbasins are composed of a lower section of submarine-fan turbidites and an upper section of shallow-water and nonmarine deltaic deposits. The aggregate thickness of the sedimentary fill in the Lower Yukon subbasin is uncertain, but regional geological and geophysical studies indicate that it may be as much as 10,000 m (Patton and Box, 1989). The thickness of the fill in the Kobuk-Koyukuk subbasin is also uncertain, but reconnaissance aeromagnetic data suggest that it is substantially less than in the Lower Yukon subbasin (Zietz and others, 1959; Dempsey and others, 1957). Petrographic studies of the deltaic sedimentary rocks in both subbasins suggest a mixed metamorphic and granitic provenance in the Ruby geanticline on the southeastern border of the basin, and paleocurrent data (Nilsen, 1989) indicate that the deltaic sediments prograded northwestward from a source on the Ruby geanticline. Deltaic deposits

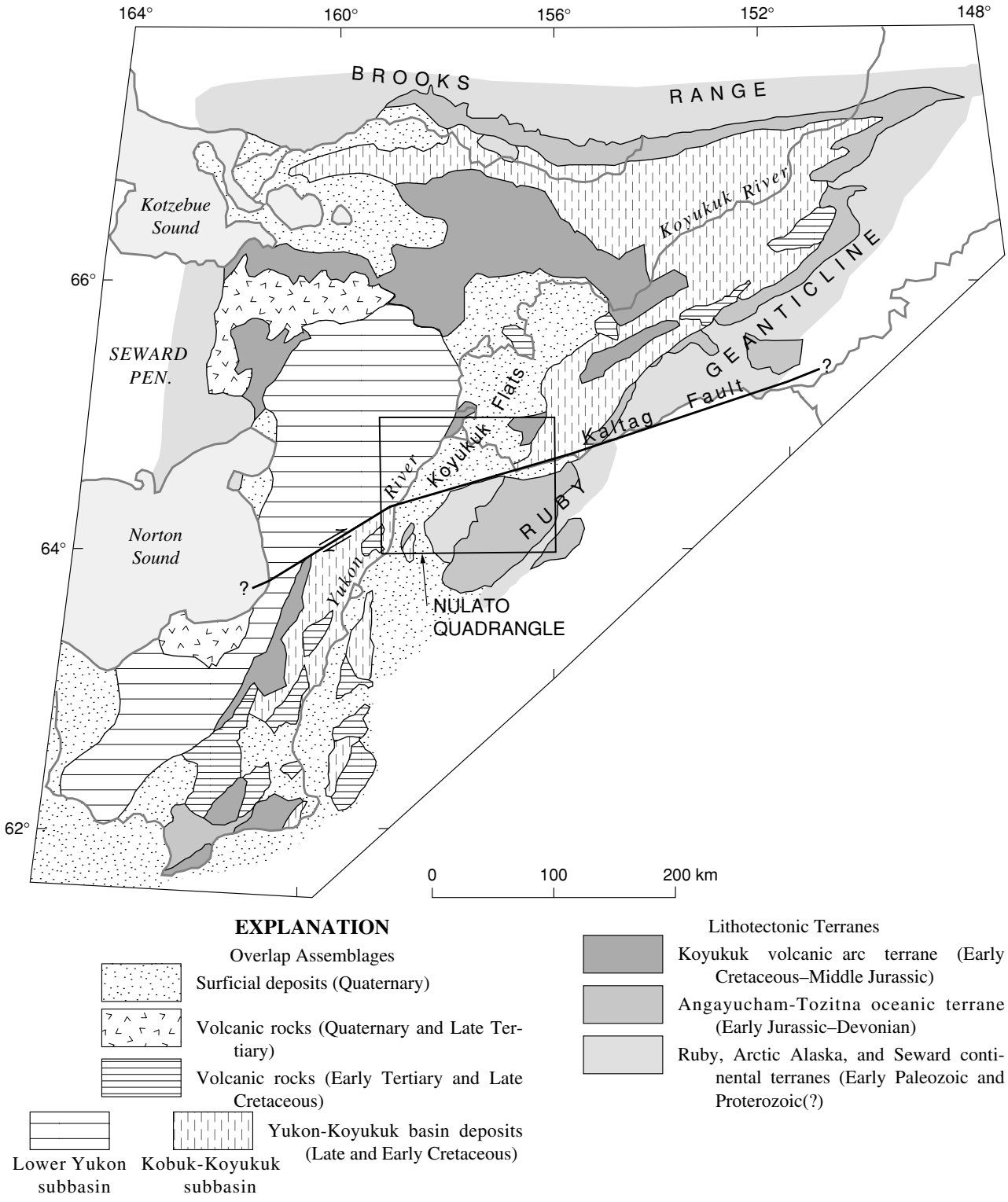

Figure 2. Generalized geologic map of the Yukon-Koyukuk basin and its borderlands showing location of Nulato quadrangle.

in the basin contain detrital white micas that yielded K-Ar ages of 131 to 158 Ma (Harris and others, 1987), about the same age as obtained from white micas in the schist and quartzite unit (PzPs) in the Kaiyuh Mountains on the Ruby geanticline (table 1).

In the Nulato quadrangle the two subbasins are separated by a broad uplift of the andesitic volca-

nic rock unit (Kv) belonging to the Koyukuk terrrane. Much of the uplift is covered by surficial deposits (map units Qfy, Qfo, Qhs) of the Koyukuk Flats, but isolated exposures of andesitic volcanic rocks crop out on the west edge of the Flats near the mouth of the Koyukuk River and on the east edge of the Flats between Bear Creek and the northern edge of the quadrangle. A single isolated exposure of the andesitic volcanic rocks forms Pilot Mountain, a prominent landmark in the Flats about 20 km west of Galena. The best evidence for the nature of the bedrock beneath the Flats is a series of aeromagnetic profiles extending northwesterly from the Koyukuk Flats across the Lower Yukon basin (Zietz and others, 1959). The profiles show steep-gradient and high-amplitude anomalies over the Flats. These anomalies indicate that highly magnetic rocks of the andesitic volcanic unit exposed at the margins of the Flats extend beneath the surficial deposits at shallow depths. The rugged aeromagnetic profiles over the Flats contrast sharply with the smooth profiles over the Lower Yukon subbasin west of the Yukon River. The margin of the Lower Yukon subbasin is sharply defined by a steep-gradient magnetic anomaly suggesting that the edge of the basin is bounded by either a fault or an abrupt wedge-out of the sedimentary section (fig. 3). The boundary anomaly can be traced northward beneath the Flats from the Kaltag Fault to a point south of the village of Nulato where it appears to be displaced by a left lateral strike-slip fault that extends northward across the Yukon River (fig. 3).

All of the Cretaceous sedimentary deposits in the Yukon-Koyukuk basin are folded and cut by numerous high-angle faults. In the Lower Yukon subbasin map units Ks and Ksm, Kcs, and Kg, representing delta, prodelta, and submarine fan facies, occur in northeast-trending belts bounded by high-angle faults. The juxtaposition of these widely different sedimentary facies suggests that the Lower Yukon subbasin has undergone early large-scale horizontal foreshortening by low-angle faults that were rotated to high-angle faults by subsequent folding or by low-angle faults that were subsequently masked by a younger system of high-angle faults. In the Lower Yukon subbasin deltaic units (Ks and Ksm) exposed along the Yukon River generally are characterized by broad open folds (Patton and Bickel, 1956)(map sheet, section *A–A′*). A short distance to the northwest in the Nulato River drainage, however, they are tightly appressed and cut by closely spaced high-angle faults, some of which show left-lateral strike-slip displacement. Further to the northwest in the Gisasa River and Arvesta Creek drainages, the prodelta and turbidite units (Kcs and Kg) are even more intensely deformed, commonly displaying overturning and isoclinal folding.

The structure of the sedimentary units Ks and Kg in the Koyukuk-Kobuk subbasin is poorly exposed and complicated by the contact effects of numerous shallow intrusive and volcanic bodies (map sheet, section *B–B′*). The best exposures are along the north bank of the Yukon River between the eastern edge of the quadrangle and the sharp bend in the river near the abandoned village of Louden. At Sandstone Bluff near the east edge of the quadrangle the deltaic unit (Ks) is mildly folded into a broad open syncline. Downstream in the vicinity of Fish Island and Bear Bluff the deltaic unit and the underlying turbidite unit (Kg) are more severely deformed and broken by numerous high-angle faults (Patton and Bickel, 1956).

Thermal maturity of sedimentary deposits in map units Ks, Ksm

Results of thermal maturation studies of the deltaic deposits (map units Ks and Ksm) in the Nulato quadrangle are shown in figure 3. Sixteen outcrop samples and a single borehole sample from a depth of 380 m in Nulato No. 1 test well were analyzed for vitrinite reflectance (percent R_o=percent reflectance in oil) (Mark Johnson, written commun., 1990; John M. Murphy, written commun., 1991; Mobil Exploration and Production Services, 1981). In order to present a complete picture of the regional distribution of the thermal maturity data in units Ks and Ksm, we also have included in figure 3 vitrinite reflectance values for nine outcrop samples from the southwestern part of the Kateel River quadrangle. The most striking feature of these data is the contrast between the low percent R_o values (0.51–1.10) along the Yukon and lower Koyukuk Rivers and the high percent R_o values (1.85–3.95) a short distance to the northwest in the same map units. For example, rocks with percent R_o values of 0.99–1.07 exposed on the Yukon River are separated by less than 15 km from percent R_o values of 3.20 and 3.04 in Nulato test well No. 1 and nearby on the South Fork of the Nulato River. Similarly, percent R_o values of 0.60 and 0.85 on the lower Koyukuk River are separated by less than 15 km from percent R_o values of 1.85 to 2.19 further north on the Koyukuk River and on the Gisasa River. The difference in thermal maturity is also reflected in the character of the deltaic deposits. The rocks of higher percent R_o values on the northwest locally display a weak slaty cleavage and are more intensely deformed and indurated than those of lower percent R_o values on the southeast. The area separating the two different sets of percent R_o values is heavily

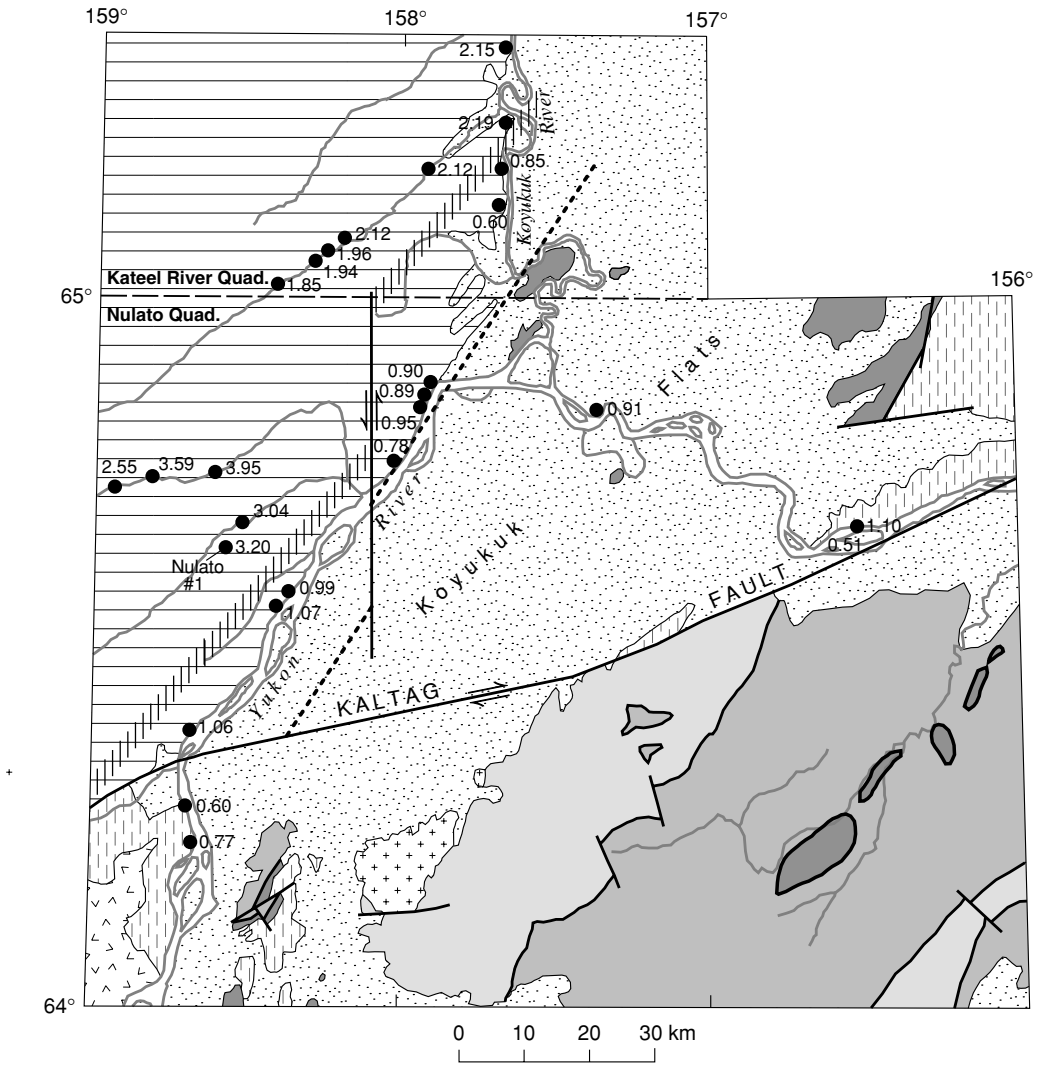

EXPLANATION

Overlap Assemblages

Surficial deposits (Quaternary)

Volcanic rocks (Tertiary)

Lower Yukon subbasin

Kobuk-Koyukuk subbasin

Yukon-Koyukuk basin sedimentary deposits (Late and Early Cretaceous)

Granitic rocks (Early Cretaceous)

Lithotectonic Terranes

Koyukuk terrane (Early Cretaceous to Middle Jurassic)

Angayucham-Tozitna terrane (Triassic to Mississppian)

Ruby terrane (Early Paleozoic and Proterozoic?)

Contact

Fault, arrows indicate direction of relative movement

● 0.91 Vitrinite reflectance (%Ro)

Boundary between high and low vitrinite reflectance values

Steep aeromagnetic gradient marking west edge of highly magnetic volcanic rocks of the Koyukuk terrane (Kv) at shallow depths (Zietz and others, 1959)

Figure 3. Generalized geologic map of the Nulato quadrangle and southwestern Kateel River quadrangle showing the location of vitrinite reflectance values for samples of the Yukon-Koyukuk basin sedimentary rocks.

vegetated and it was not possible to determine if the abrupt change in thermal maturity reflects juxtaposition by faulting or a rapid change in the paleothermal gradient. The boundary between the two sets of percent R_o values appears to parallel a steep aeromagnetic gradient marking the edge of the highly magnetic andesitic volcanic unit (Kv) that underlies the Koyukuk Flats (Zietz and others, 1959; Dempsey and others, 1957). Both the steep aeromagnetic gradient and the boundary between the high and low thermal maturity values appear to be offset by a north-trending left-lateral strike-slip fault that extends across the Yukon River (fig. 3).

RUBY GEANTICLINE

The Ruby geanticline is a broad mid-Cretaceous uplift that borders the Yukon-Koyukuk basin on the southeast and extends diagonally southwestward across central Alaska from the Brooks Range to beyond the southern edge of the Nulato quadrangle (fig. 1). The core of the geanticline consists of the early Paleozoic and Proterozoic (?) continental margin deposits of the Ruby terrane (map units PzPs, Pzc, PzPm) that were metamorphosed to greenschist, blueschist, and amphibolite facies in Mesozoic time. Structurally overlying the Ruby terrane are allochthonous bodies of late Paleozoic and early Mesozoic oceanic rocks of the Angayucham-Tozitna terrane (map units TrMb, TrMq) and small Late and Middle Jurassic mafic-ultramafic complexes belonging to the Koyukuk volcanic-arc terrane (map units Juu, Jcu, Jht) (map sheet, sections *C–C′*, *D–D′*). The rocks of the Ruby geanticline are widely intruded and thermally altered by large mid-Cretaceous granitoid plutons such as the Khotol pluton (map unit Kgr) in the Nulato quadrangle. The intrusive event clearly post-dated regional metamorphism of the Ruby terrane and emplacement of the allochthonous Angayucham-Tozitna and Koyukuk terranes.

The Ruby geanticline is interpreted as a subduction-related imbricated assemblage of continental-margin, oceanic and volcanic-arc thrust slices emplaced in Middle and Late Jurassic time when the Koyukuk volcanic-arc terrane collided with the Ruby continental-margin terrane (Patton and Box, 1989). In the Kaiyuh Mountains the thrust fault contact between the Ruby terrane (map units PzPs, Pzc, PzPm) and Angayucham-Tozitna terrane (map units TrMb, TrMq) can be traced from the southern border of the quadrangle northeastward to the Kaltag Fault. The contact is marked by a highly tectonized zone of ductily deformed, blueschist-greenschist facies pelitic schist, quartzite, carbonate rocks, and metabasite. It is offset about 5 km in two places by left lateral northwest-trending strike-slip faults. Other thrust faults may be present within the Ruby terrane, but have not been recognized owing to lack of continuous exposures. Some of the thin bodies of the carbonate rock (Pzc) unit and the metabasite (PzPm) unit may represent separate thrust slices. Unrecognized thrust slices also may exist within the Angayucham-Tozitna terrane. The abrupt eastward transition from strongly foliated blueschist-greenschist metamorphic facies rocks in the basalt and gabbro (TrMb) unit in the Kaiyuh Mountains to low greenschist and zeolite facies rocks in the Yuki River drainage suggests that the two metamorphic facies may have been juxtaposed by thrust faulting. In the Yuki River drainage the basalt, gabbro, and chert unit (TrMb) of the Angayucham-Tozitna terrane is overlain by klippen of the ultramafic-mafic complexes of the Koyukuk terrane (map units Juu, Jcu, Jht). The thrust fault at the base of the klippen, which is exposed in two places, is marked by a highly tectonized zone of strongly layered garnet amphibolite and pyroxene granulite. In the southeastern corner of the quadrangle the Ruby and Angayucham-Tozitna terranes are poorly exposed and little is known about their structure. Contacts between the basalt, gabbro, and, chert unit (TrMb), the quartzite, phyllite, and limestone unit (TrMq), and the schist and quartzite unit (PzPs) appear to be high-angle faults.

The direction of tectonic transport for the thrust sheets of the Ruby geanticline is controversial. On the map sheet in sections *C–C′* and *D–D′*, we show a top-to-the-southeast direction of tectonic transport following the model proposed by Patton and Box (1989). This model suggests that the Ruby terrane was subducted beneath the oceanic and volcanic arc rocks of the Angayucham-Tozitna and Koyukuk terranes along a northwest-dipping subduction zone. A different model, however, has been suggested by Roeske and McClelland (1997) on the basis of their S-C fabric studies of the thrust faulted contact of the Ruby and Angayucham-Tozitna terranes at several localites in the Kaiyuh Mountains. They interpret these metamorphic fabrics to indicate that tectonic transport was top-to-the-northwest and they favor a subduction model that employs a southeast-dipping subduction zone.

KALTAG FAULT

The Kaltag Fault slices diagonally across the Nulato quadrangle and offsets the Yukon-Koyukuk basin and Ruby geanticline right-laterally 100 to 130 km (figs. 1 and 2). The fault enters the western edge of the Nulato quadrangle along a narrow fault-line valley that cuts across northern tributaries of the Kaltag River. The trace of the fault is

clearly marked by diverted streams, offset spurs, and fault-bounded bedrock slivers. Beheaded tributaries along this stretch show right-lateral stream offsets of 1 to 2.5 km (Patton and Hoare, 1968). About 8 km west of the village of the Kaltag the fault emerges from the fault-line valley, crosses the alluviated lowlands of the Kaltag River, and intersects the Yukon River about 1.5 km north of the village. East of the Yukon River the fault is inferred to extend across a broad expanse of older

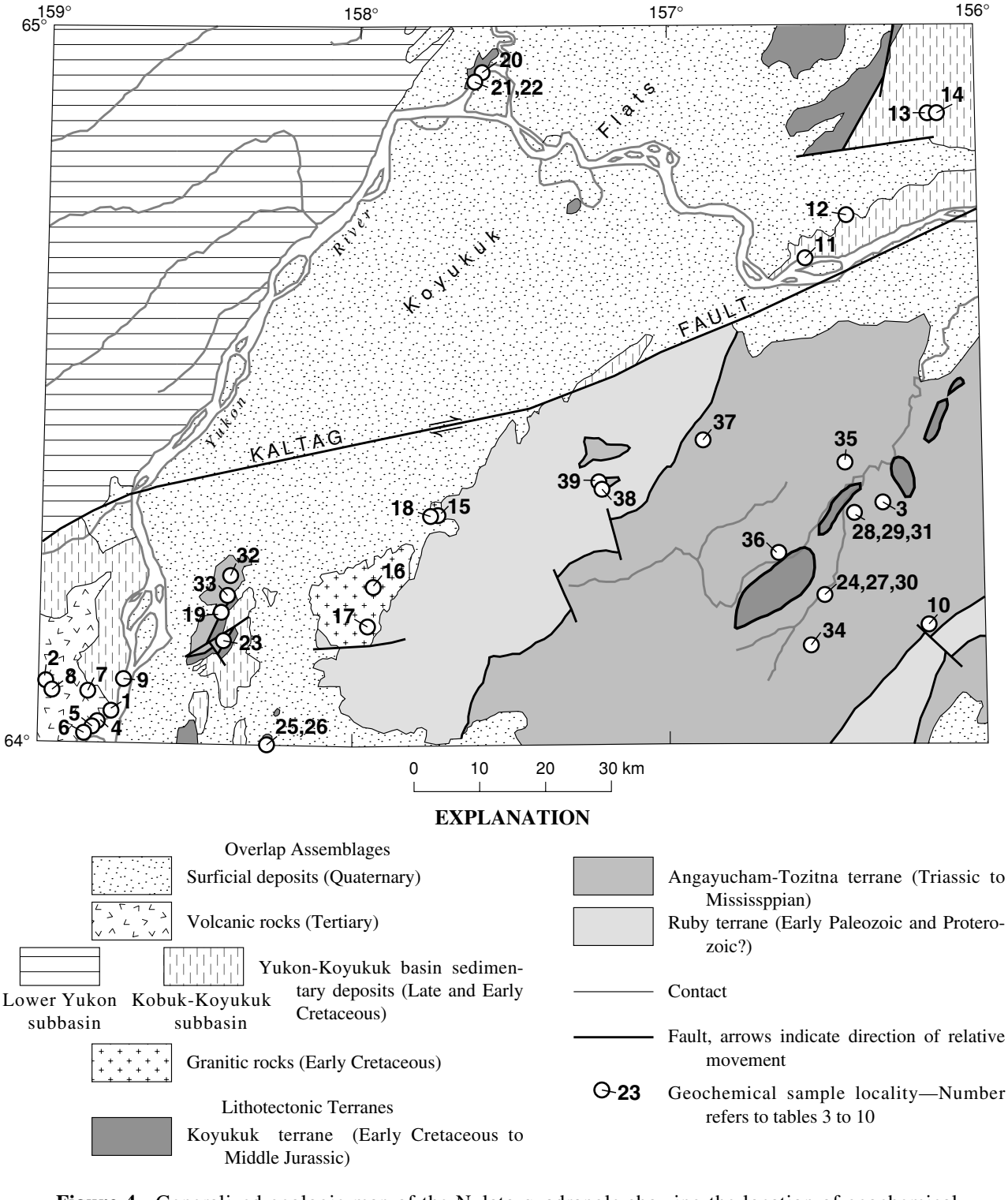

Figure 4. Generalized geologic map of the Nulato quadrangle showing the location of geochemical samples listed in tables 3–10.

flood-plain deposits (Qfo) at the southern edge of the Koyukuk Flats. Only a few faint traces of the fault are visible in aerial photographs along this segment. However, the Flats along this segment appear to have sunk recently as evidenced by ponded drainages and numerous coalescing thaw lakes. Active sinking is also suggested by the presence of a –20 mGal isostatic gravity anomaly centered over this part of the Flats (Barnes and others, 1994). About 65 km east of the Yukon River the fault bends to a slightly more northerly course and follows along the base of the Kaiyuh Mountains as far as the mouth of Kala Creek. The trace of the fault along this segment is clearly marked in aerial photographs by a thin line of heavy vegetation and scarplets cutting across the high terrace and slope deposits (Qhs). A ridge of deltaic (Ks) and turbidite deposits (Kg) of Yukon-Koyukuk basin trends at an acute angle into the fault on the northwest side and is opposed on the southeast side by schist and quartzite (PzPs) of the Ruby terrane. The fault leaves the Kaiyuh Mountains and enters the Yukon valley at the sharp bend in the Yukon River near the abandoned village of Louden. From this point it continues northeastward along the straight-line course of the Yukon River for another 200 km, well beyond the eastern edge of the Nulato quadrangle.

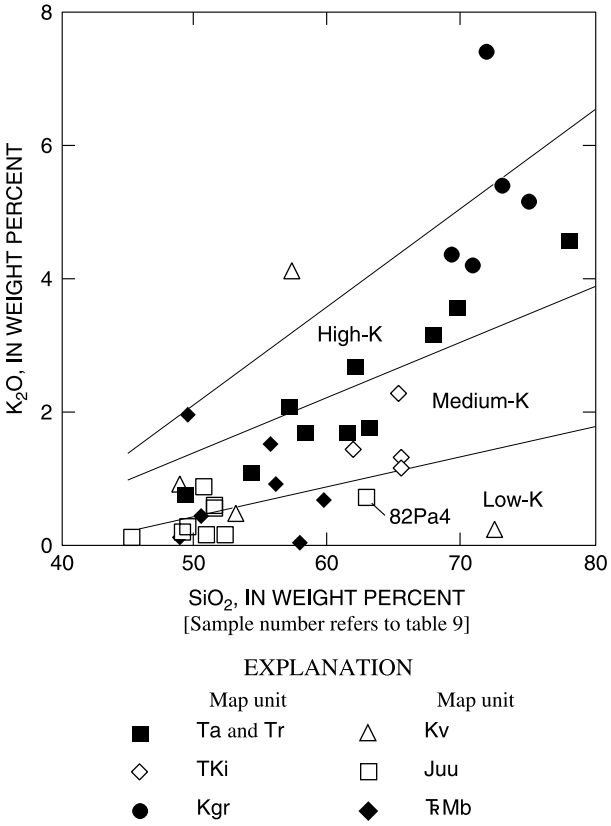

Figure 5. Plot of K_2O compared to SiO_2 for map units from the Nulato quadrangle, west-central Alaska. Most of the suites show increasing K_2O with increasing SiO_2. Boundaries for high-K, medium-K, and low-K extended from fields given in Gill (1981). The early Tertiary volcanic rocks (map units Ta and Tr) are medium to high K. The early Tertiary and Late Cretaceous shallow intrusive rocks (map unit TKi) are medium K. Samples from the Early Cretaceous Khotol pluton (map unit Kgr) have high to very high potassium. The Early Cretaceous arc volcanic rocks (map unit Kv) show an extreme variation in K, probably due to alteration, and plot in the low-K and very high-K fields. Samples from map unit Juu plot in the low- or medium-K field. Sample 82Pa4 is tentatively assigned to map unit Juu but is of uncertain affinities. The Angayucham-Tozitna terrane samples in map unit TrMb plot in the medium-K field. See Description of Map Units for explanation of map unit symbols.

GEOCHEMICAL CHARACTERISTICS OF VOLCANIC AND PLUTONIC ROCK UNITS

The rocks exposed in the Nulato quadrangle record a long complex magmatic history beginning in the Paleozoic and continuing into the early Tertiary. Samples from all magmatic units were analyzed for major and trace-element composition (tables 3–10). Sample locations are shown on figure 4, and their composition and tectonic affinities are discussed below. Nomenclature used in this paper generally follows that of Streckeisen (1979) and Gill (1981). Major oxides are normalized to 100 percent dry weight (without water and CO_2) before classification and plotting. On an anhydrous basis, basalts have less than 52 percent SiO_2, andesites have 53 to 63 percent SiO_2, dacites have 63 to 70 percent SiO_2, and rhyolites have more than 70 percent SiO_2. Fe_2O_3/FeO was set to 0.30 where FeO was not analyzed.

EARLY TERTIARY AND LATE CRETACEOUS ROCKS

Andesite and basalt (Ta), rhyolite and dacite (Tr), and shallow intrusive rocks (TKi)

Discontinuous outcrops of early Tertiary and Late Cretaceous volcanic and intrusive rocks occur throughout western Alaska. These outcrops are all that remain of a vast magmatic province that once extended from the Arctic Circle south to Bristol Bay and west to St. Matthew Island in the Bering Sea (Moll-Stalcup, 1994). Rocks from the early Tertiary-Late Cretaceous magmatic province are sparsely exposed in the Nulato quadrangle and have not been

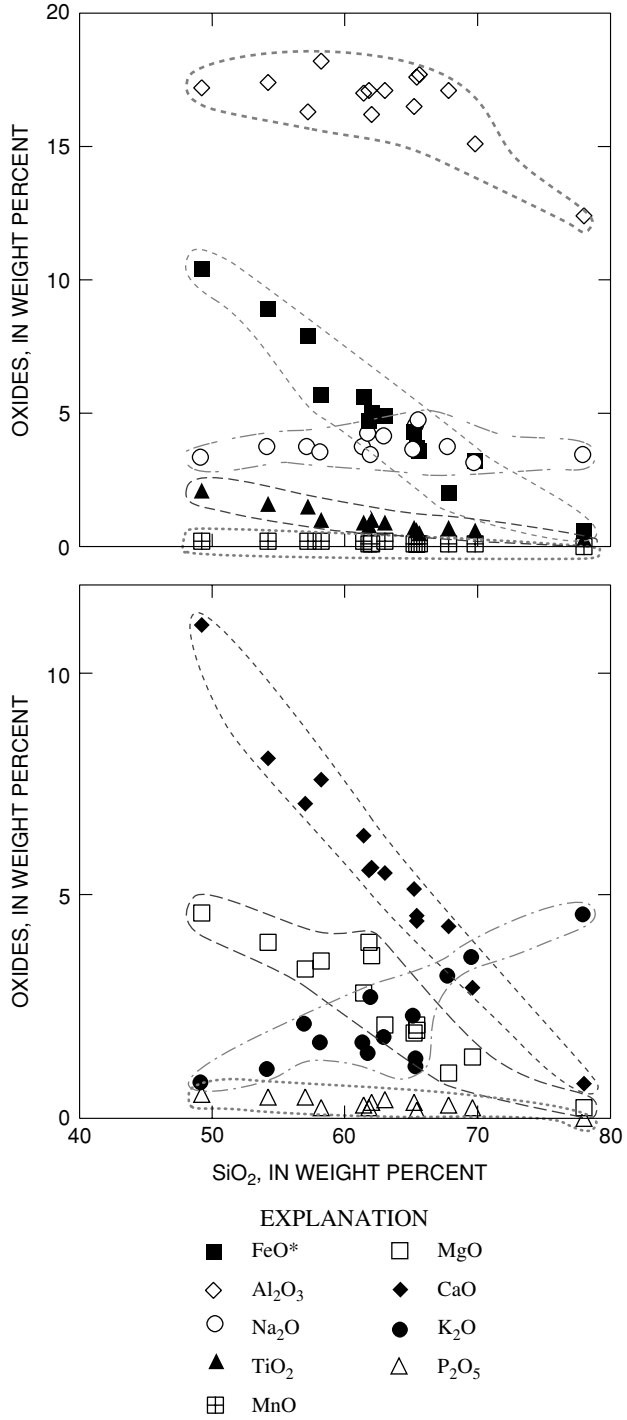

Figure 6. Plots of major-element oxides against SiO_2 for early Tertiary and Late Cretaceous volcanic and intrusive rocks (map units Tr, Ta, TKi) of the Nulato quadrangle, west-central Alaska.

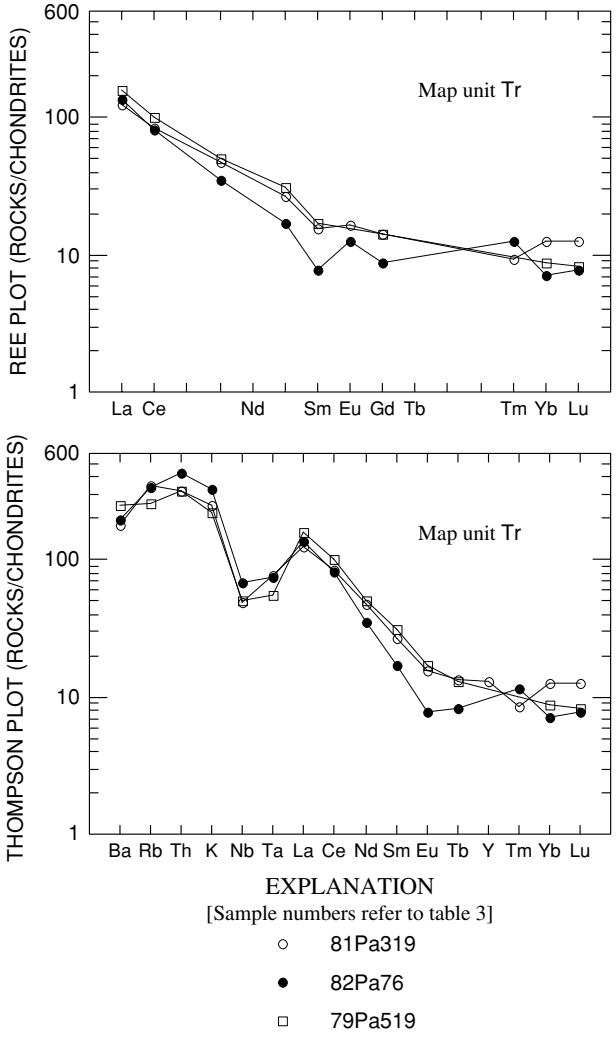

Figure 7. Plots of rare earth elements (REE) and trace elements for rhyolite and dacite samples from unit Tr. The three samples have similar patterns, except the rhyolite (82Pa76) has a larger negative Eu anomaly than the two dacites. Data in trace-element plot normalized to values given in Thompson and others (1984) and plotted using program of Wheately and Rock (1988). See Description of Map Units for explanation of map unit symbols.

studied in detail. However, volcanic and intrusive rocks of similar composition and age have been studied in considerable detail in Blackburn Hills, 60 km to the southwest in the Unalakleet quadrangle (Moll-Stalcup and Patton, 1992; Moll-Stalcup and Arth, 1989). Chemical analyses of the Nulato quadrangle rocks are limited to three samples from map unit Tr, seven samples from map unit Ta, and four samples from map unit TKi (tables 3–5). Early Tertiary and Late Cretaceous volcanic and intrusive rocks in the Nulato quadrangle consist of a compositionally coherent suite of basalt, andesite, dacite, and rhyolite. Samples from the Nulato quadrangle have between 48 and 76 percent SiO_2 (49 and 78 percent, anhydrous) and are medium- to high-K calc-

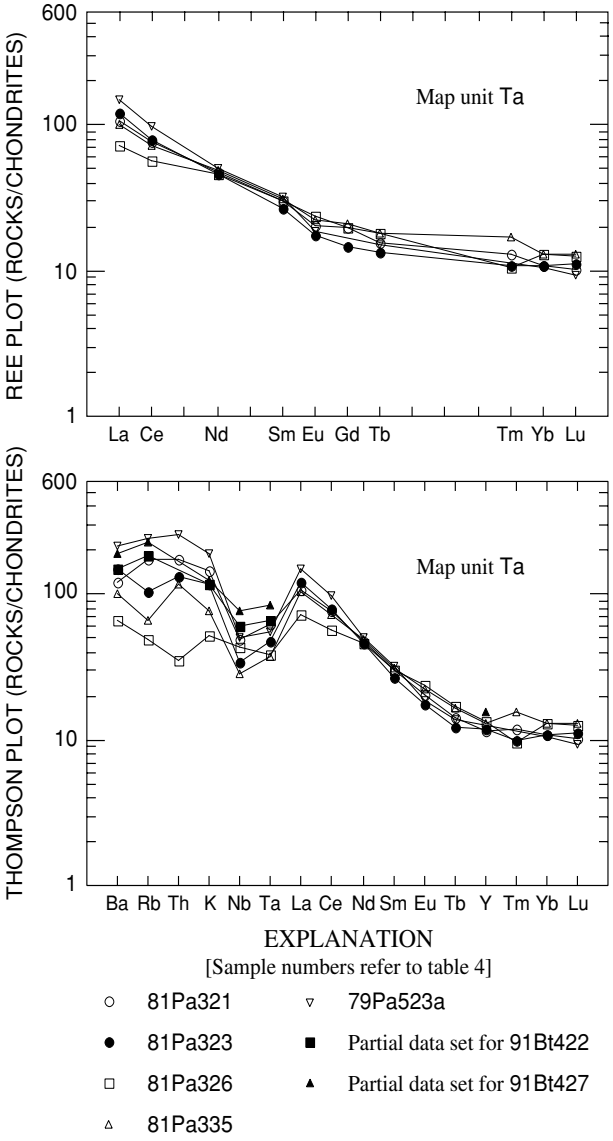

Figure 8. Plots of rare earth elements (REE) and trace elements for basalt and andesite samples from unit Ta. All of the andesites have enriched alkali elements (Ba, Rb, Th, and K) and LREE (La, Ce) relative to Nb and Ta, a pattern that is typical of arc-related rocks. The lower alkali element and LREE contents relative to Nb and Ta of the only basalt (81Pa326) suggest the basalt may be part of a post-subduction suite. Data in trace-element plot normalized to values given in Thompson and others (1984) and plotted using program of Wheately and Rock (1988). See Description of Map Units for explanation of map unit symbols.

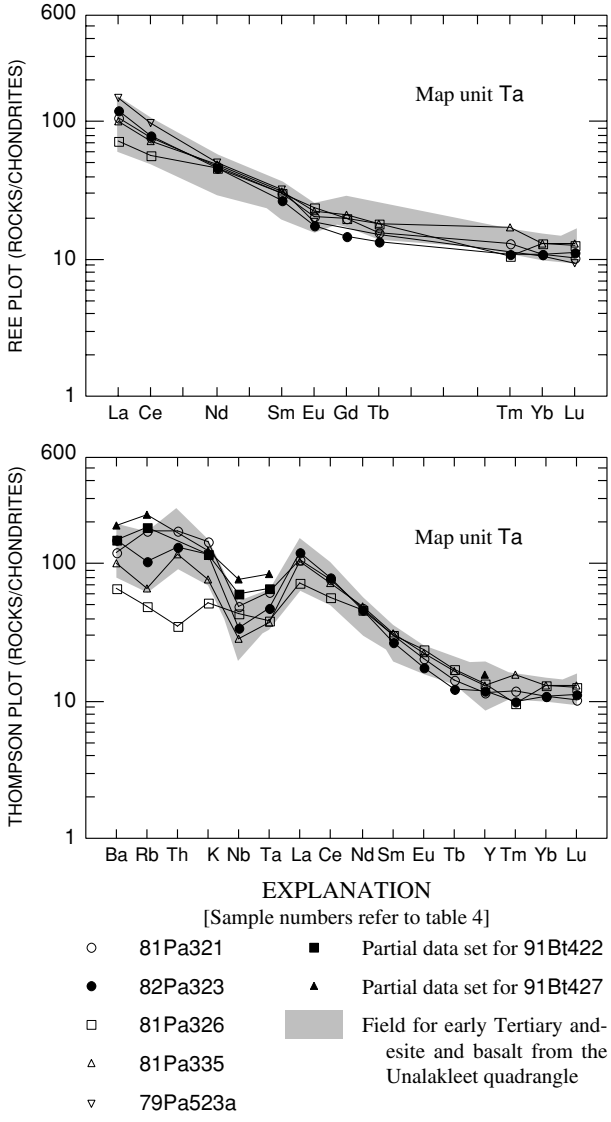

Figure 9. Plots of rare earth elements (REE) and trace elements for early Tertiary andesite and basalt (map unit Ta) in the Nulato quadrangle compared with data for early Tertiary andesite and basalt in the Unalakleet quadrangle (shaded area). Data from both areas are strikingly similar. Data in trace-element plot normalized to values given in Thompson and others (1984) and plotted using program of Wheately and Rock (1988). See Description of Map Units for explanation of map unit symbols.

alkalic (fig. 5). FeO, TiO_2, Al_2O_3, CaO, MgO and P_20_5 decrease with increasing SiO_2, while Na_2O remains nearly constant and K_2O increases (fig. 6) similar to calc-alkalic suites worldwide. Basalt, andesite, dacite, and rhyolite from map units Ta and Tr are light rare-earth element (LREE) enriched, and show negative Nb and Ta anomalies on plots (figs. 7 and 8) similar to early Tertiary volcanic rocks from the Blackburn Hills in the adjoining Unalakleet quadrangle (fig. 9). Alkali elements are enriched and Nb and Ta are depleted relative to the LREE, patterns typical of subduction-related

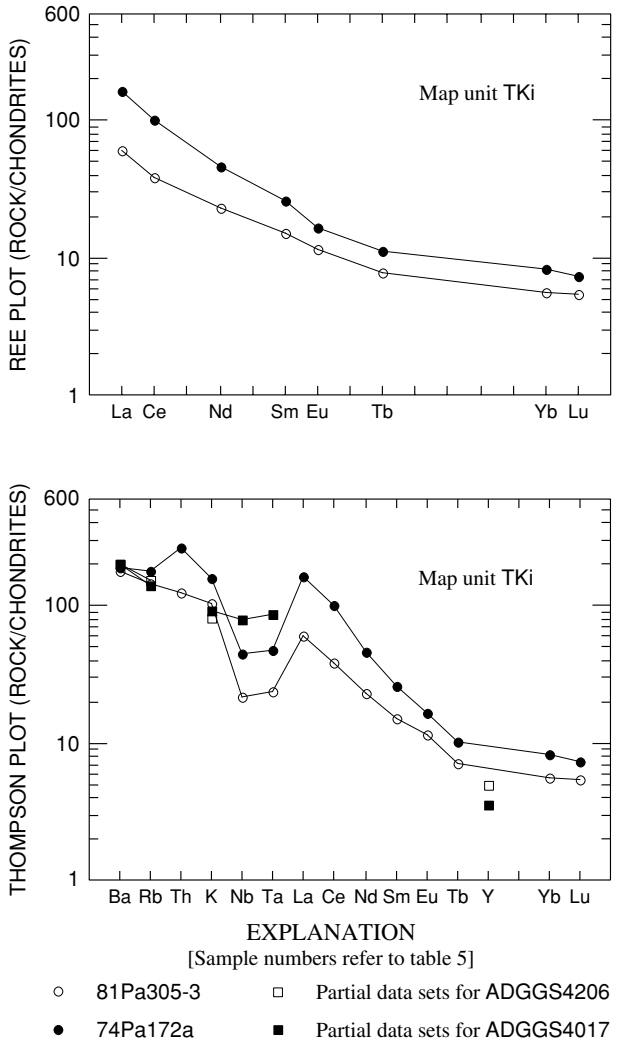

Figure 10. Plots of rare earth elements (REE) and trace elements for samples of early Tertiary and Late Cretaceous rocks (map unit TKi). Data in trace-element plot normalized to values given in Thompson and others (1984) and plotted using program of Wheately and Rock (1988). See Description of Map Units for explanation of map unit symbols.

magmatism (figs. 7, 8, and 9). One sample of basalt from map unit Ta (fig. 8, 81Pa326) shows no depletion in Nb and Ta relative to alkali elements and little depletion in Nb and Ta relative to the LREE. In this respect it is similar to basalts elsewhere in western Alaska that generally are restricted to the top of the stratigraphic section and have been interpreted to represent the waning stages of subduction-related magmatism. The Nulato sample, however, is not alkalic and differs in this respect from the higher level basalts in other parts of western Alaska, which are usually mildly alkalic.

Two dacite samples and one rhyolite sample from map unit Tr are high-K calc-alkalic (table 3). On the rare-earth-element (REE) and trace-element plots (fig. 7), the three felsic samples have patterns similar to andesites of unit Ta, but have higher alkali element contents. The rhyolite has a larger negative Eu anomaly than the dacites or andesites.

The early Tertiary and Late Cretaceous shallow intrusive rocks of map unit TKi have a narrow range of 60 to 63 percent SiO_2 (62 to 65 percent, anhydrous) and are medium-K calc-alkalic (table 5). The two samples that were analyzed for REE, are LREE enriched and show negative Nb and Ta anoma-

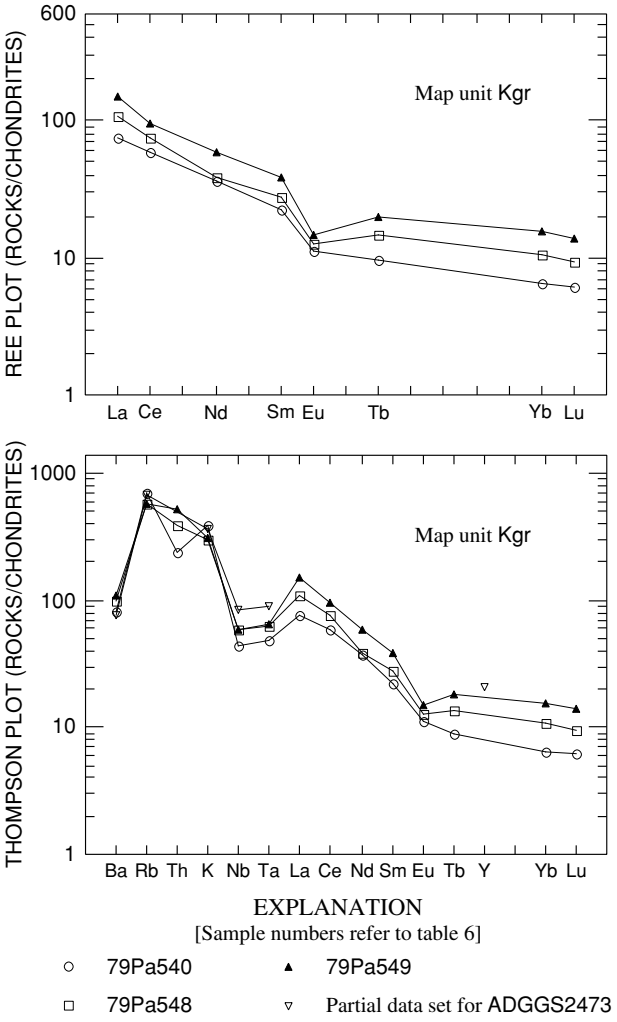

Figure 11. Plots of rare earth elements (REE) and trace elements for samples of Early Cretaceous granite from the Khotol pluton (map unit Kgr). Data in trace-element plot normalized to values given in Thompson and others (1984) and plotted using program of Wheately and Rock (1988). See Description of Map Units for explanation of map unit symbols.

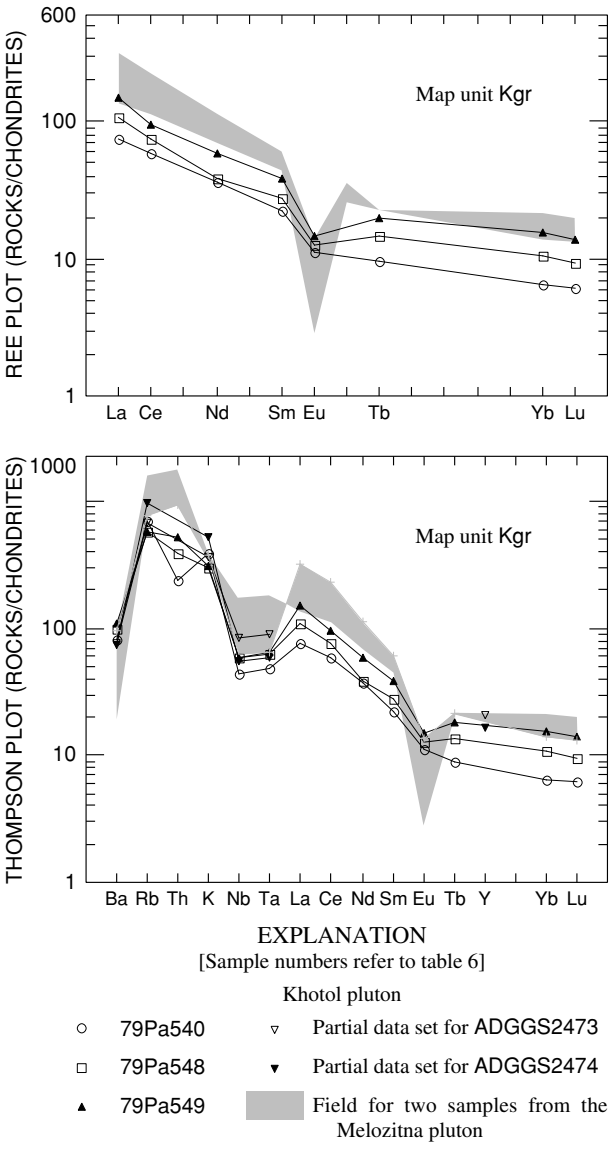

Figure 12. Plots of rare earth elements (REE) and trace elements for samples from of Early Cretaceous granite from the Khotol pluton (map unit Kgr) in the Nulato quadrangle compared with samples from the Melozitna pluton in the Melozitna quadrangle (shaded area). The two samples from the Melozitna pluton appear to be chemically similar but more evolved than those from the Khotol pluton. Data in trace-element plot normalized to values given in Thompson and others (1984) and plotted using the program of Wheately and Rock (1988). See Description of Map Units for explanation of map unit symbols.

lies on the trace-element plots (fig. 10) similar to the rocks of units Tr and Ta (figs. 7 and 8). In contrast to samples from units Ta and Tr, the two TKi samples show patterns that are slightly more concave downward and have lower Y, Yb, and Lu content (fig. 10). Patterns like these often indicate amphibole fractionation, but amphibole was recognized in only one of the samples (74Pa172a).

EARLY CRETACEOUS ROCKS

Granite (Kgr) of the Khotol pluton

Four samples from the Khotol pluton show little variation in major- or trace-element content (table 6). The samples have between 68 and 75 percent SiO_2 (69 and 75 percent, anhydrous), 4.1 and 5.3 percent K_2O (4.2 and 5.4 percent, anhydrous), 155 and 197 ppm Sr, and 525 and 742 ppm Ba. The pluton is characterized by high K_2O/Na_2O ratios. REE patterns are LREE enriched and have small Eu anomalies (fig. 11). Trace-element plots have shapes similar to arc volcanic rocks, but the Khotol plutonic rocks have higher Rb, Th, and K contents and, in the case of one sample, lower Y, Yb, and Lu contents than typical arc rocks.

It has been suggested that the Khotol pluton is the southern lobe of the Melozitna pluton that has been right-laterally offset by the Kaltag Fault about 160 km to its present position (Patton and others, 1984). The Melozitna pluton is located on the north side of the Kaltag fault in the Melozitna quadrangle, northeast of the Nulato quadrangle. Two samples from the Melozitna pluton analyzed by Arth and others (1989) and Miller (1989) for major and trace elements are compositionally similar to the Khotol pluton (table 7), although one of the Melozitna samples has significantly higher Rb and Th and lower Ba, Sr, Co, and Cr contents than the other Melozitna sample or the Nulato samples. The Melozitna samples appear more evolved because they have deeper negative Eu anomalies and have higher alkali-element and LREE contents (fig. 12). There are insufficient data from either pluton to make a definitive correlation between the two plutons on the basis of the chemical data.

EARLY CRETACEOUS AND LATE AND MIDDLE JURASSIC ROCKS

Andesitic volcanic rocks (Kv) of the Koyukuk terrane

Four samples from the andesitic volcanic unit (Kv) in the Nulato quadrangle were analyzed for chemical content (table 8). Duplicate analyses were obtained for trace elements for two of the samples. All four of the analyzed samples are highly altered and three of the samples contain more than 6 percent LOI (lost on ignition) or combined water and CO_2. The four samples have between 45 and 71

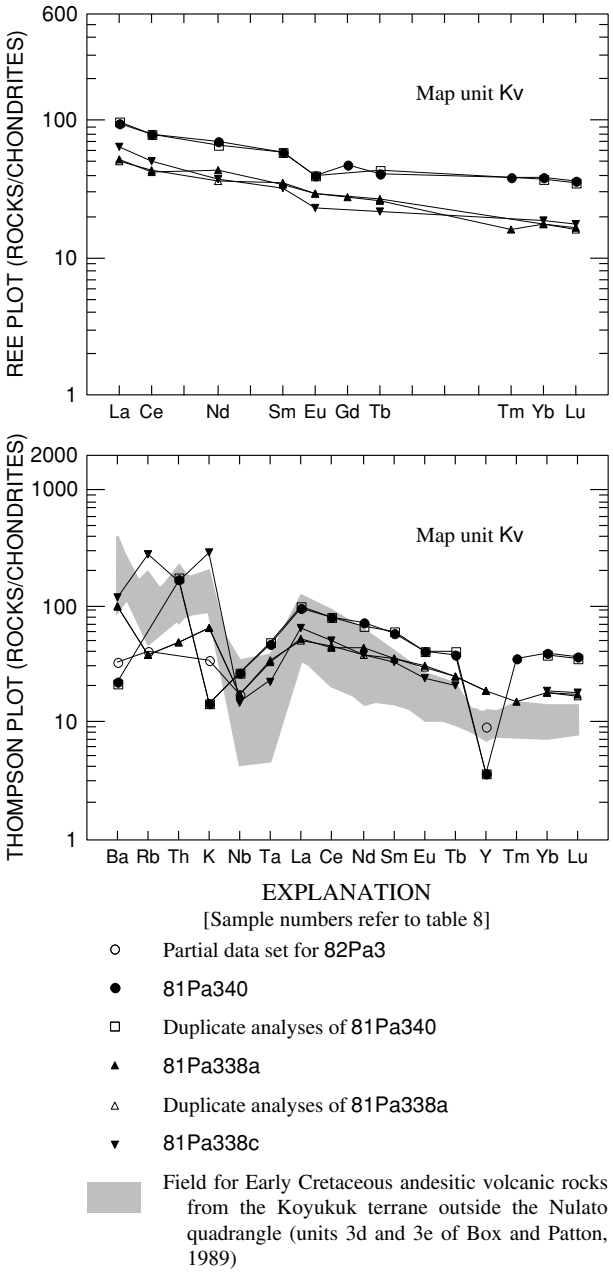

Figure 13. Plots of rare earth elements (REE) and trace elements for samples from Early Cretaceous andesitic volcanic rocks map unit of the Koyukuk terrane (Kv). Two samples were analyzed twice, once in 1993 with the earlier data set and once in 1995. The plots show good agreement between the two sets of data. The shaded field compares data for map unit Kv with the more extensive data for Early Cretaceous andesitic volcanic rocks in the Koyukuk terrane outside the Nulato quadrangle (data from Box and Patton, 1989). Data in trace-element plot normalized to values given in Thompson and others (1984) and plotted using the program of Wheately and Rock (1988). See Description of Map Units for explanation of map-unit symbols.

percent SiO_2 (49 and 72 percent, anhydrous); alkali elements, especially K, are so altered as to be considered unreliable. REE data from three samples have LREE enriched patterns (samples 81Pa338a, 338c, and 340, fig. 13). Trace-element plots show erratic patterns in the alkalis (Ba, Rb, Th, K) due to alteration and slightly higher Ta values than expected relative to their Nb values (fig. 13). Sample 81Pa340 has an unexplained low Y content. The Nulato samples appear broadly similar but more altered when compared to data from Box and Patton (1989) for Early Cretaceous andesitic volcanic rocks (units 3d and 3e) of the Koyukuk terrane from elsewhere in west-central Alaska (fig. 13).

Using their more extensive data set, Box and Patton (1989) concluded that the Koyukuk terrane was part of an intraoceanic island arc that collided with the continental margin of western Alaska beginning about 145 Ma. The chemical data from the Nulato quadrangle are consistent with an intraoceanic arc setting for the andesitic volcanic rocks of map unit Kv.

Ultramafic-mafic complexes (Juu, Jcu, Jht)

Although the ultramafic-mafic complexes in the Nulato quadrangle consist largely of ultramafic rocks, sampling for chemical analyses was confined to the less abundant, but tectonically more significant mafic component. Of the nine samples shown in table 9, three are gabbro, five are amphibolite, and one is a diorite. The three gabbro samples have REE patterns that are slightly LREE enriched (fig. 14). The five amphibolite samples have flat or LREE-depleted REE patterns. Three of the amphibolite samples have small positive Eu anomalies, which usually indicates plagioclase accumulation. None of the samples was analyzed for Nb and only four samples were analyzed for Ta. The three gabbro samples (74Pa127c, 79Pa180b, and 74Pa552a) have small Nb-Ta anomalies (Nb content is calculated assuming Ta x 16=Nb, after Gill, 1981); the one amphibolite sample analyzed for Ta (74Pa127a) shows no Nb-Ta anomaly.

A single diorite sample (82Pa4) was collected from an isolated outcrop in the Magitchlie Range. The geologic affinities of this outcrop are uncertain and it may not be part of an ultramafic-mafic complex. The sample has more SiO_2 than the other samples in this unit (table 9; fig. 5) and possibly is related to a trondhjemite and tonalite unit that is widely exposed in the Koyukuk terrane in the adjoining Unalakleet quadrangle (Patton and Moll-Stalcup, 1996).

Recent studies (Patton, 1993) suggest that the ultramafic-mafic complexes belong in Koyukuk vol-

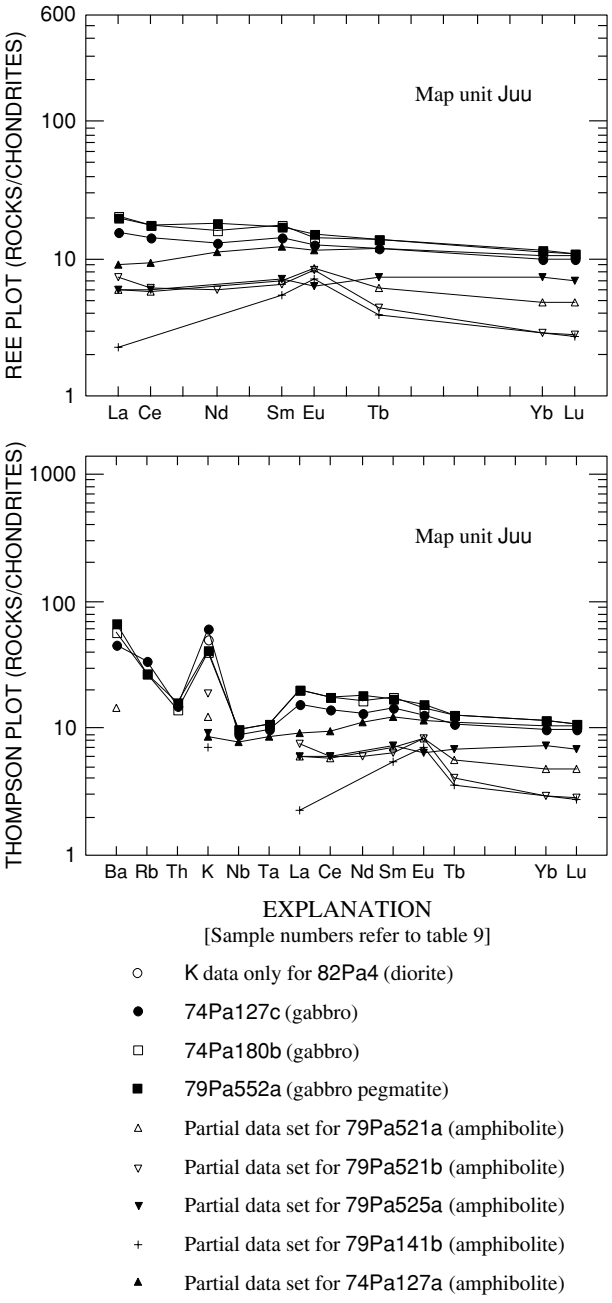

Figure 14. Plots of rare earth elements (REE) and trace elements for samples from Late and Middle Jurassic ultramafic-mafic complexes of the Koyukuk terrane (map unit Juu). Data in trace-element plot normalized to values given in Thompson and others (1984) and plotted using program of Wheately and Rock (1988). See Description of Map Units for explanation of map unit symbols.

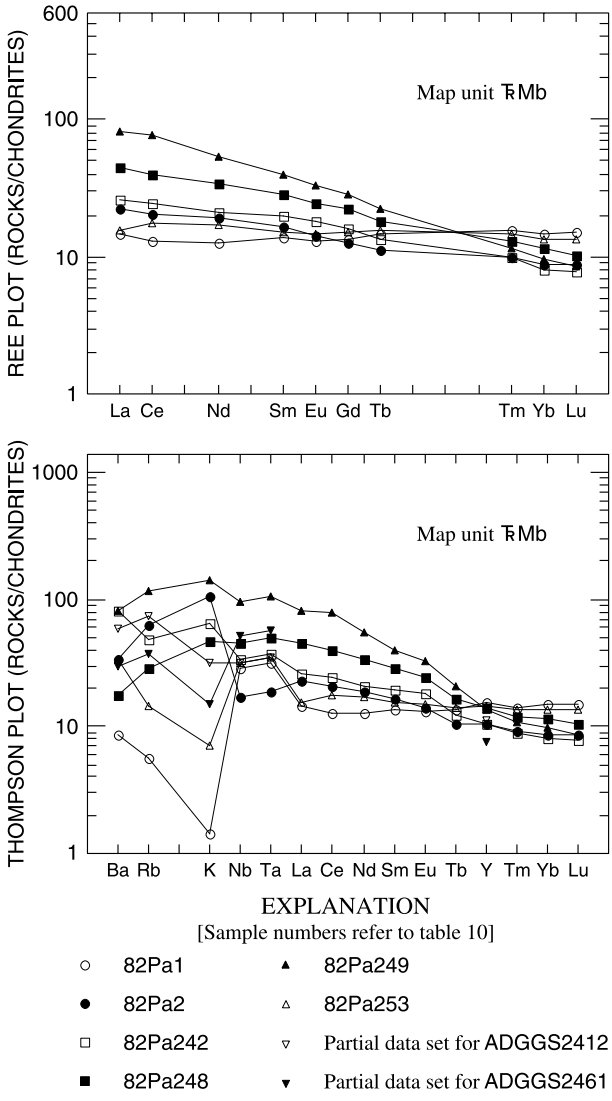

Figure 15. Plots of rare earth elements (REE) and trace elements for samples from the Triassic to Mississippian altered basalt, gabbro, and chert map unit of the Angayucham-Tozitna terrane (TrMb). Data in trace-element plot normalized to values given in Thompson and others (1984) and plotted using program of Wheately and Rock (1988). See Description of Map Units for explanation of map unit symbols.

canic-arc terrane rather than in the Angayucham-Tozitna oceanic terrane, as previously thought. The gabbro and gabbro pegmatite dikes have Nb and Ta anomalies on trace-element plots which suggest they may be veins of arc-related fluid injected into the mantle, possibly during the oldest stage of Koyukuk arc magmatism. One amphibolite sample, however, has a flat REE pattern with no negative Nb and Ta anomaly and is more indicative of an ocean-floor environment than of an island-arc environment (fig. 14).

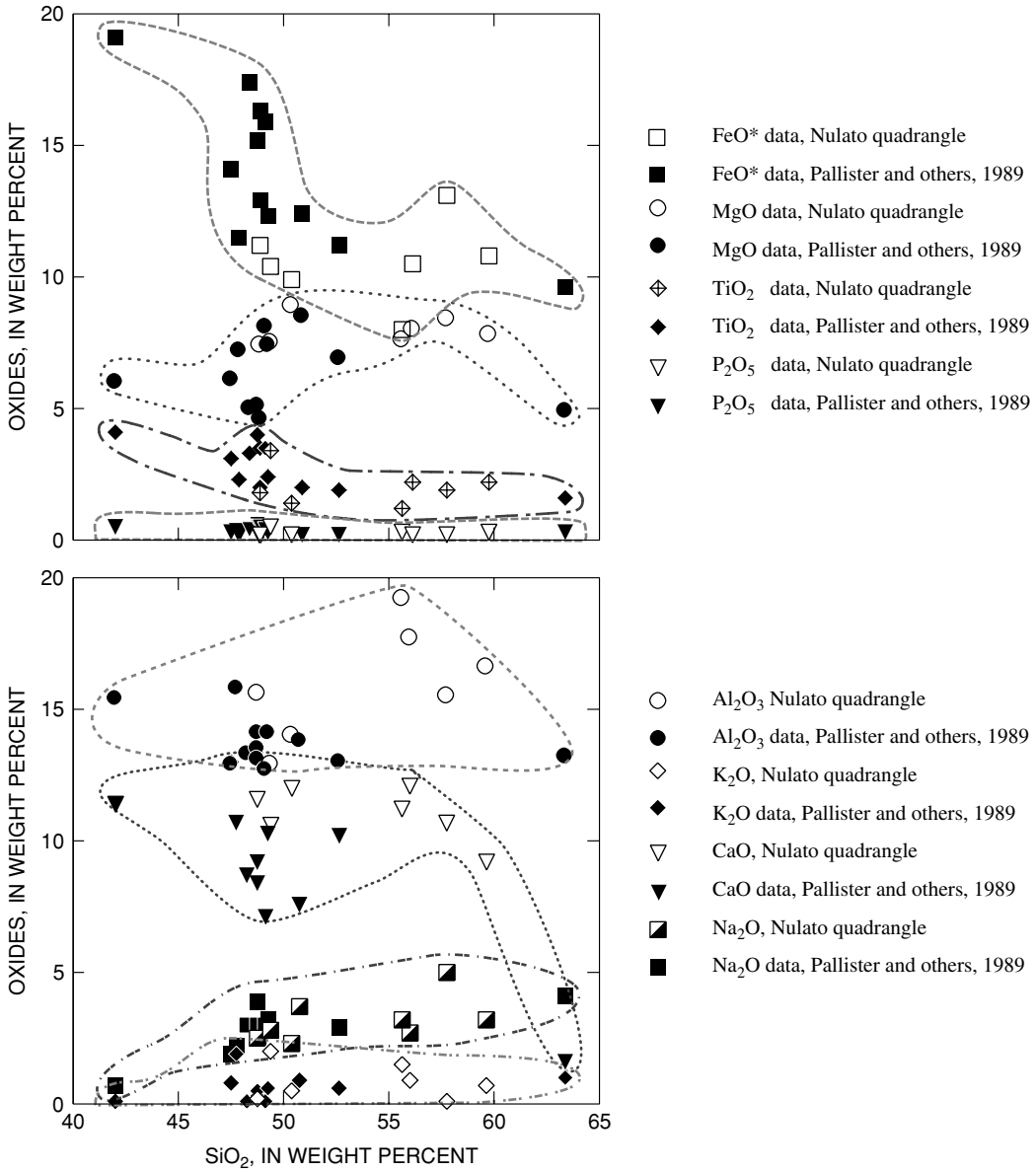

Figure 16. Plots of major-element oxides against SiO_2 for samples from the Triassic to Mississippian basalt, gabbro, and chert map unit of the Angayucham-Tozitna terrane (TRMb) in the Nulato quadrangle, west-central Alaska compared to data as given in Pallister and others (1989) for Jurassic to Triassic basalt in the Angayucham terrane of the Brook Range on the northern margin of the Yukon-Koyukuk basin (fig. 2).

TRIASSIC TO MISSISSIPPIAN ROCKS

Altered basalt, gabbro, and chert (TRMb) of the Angayucham-Tozitna terrane

Eight samples of basalt and diabase from the altered basalt, gabbro, and chert map unit (TRMb) of the Angayucham-Tozitna terrane were analyzed for major and trace elements (table 10). All of the samples are highly altered and have undergone varying degrees of regional metamorphism. Although some of the samples have more than 53 weight percent SiO_2, when calculated on a volatile-free basis, all appear to be of basaltic composition because they have at least 6.5 percent MgO when calculated on a volatile-free basis.

Samples from map unit TRMb in the Angayucham-Tozitna terrane in the Nulato quadrangle have flat to LREE-enriched REE patterns (fig.

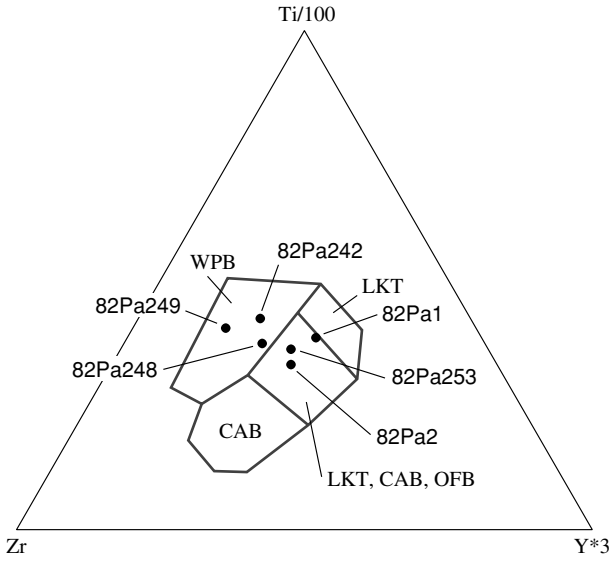

Figure 17. Pearce-Cann plot for samples from the Triassic to Mississippian basalt, gabbro, and chert map unit of the Angayucham-Tozitna terrane (TrMb) in the Nulato quadrangle, west-central Alaska. Sample numbers refer to table 10. Plots like these use relatively immobile elements to distinguish basaltic rock formed in different tectonic environments. Field abbreviations: WPB, within-plate basalt (oceanic or continental); LKT, low-potassium tholeiite; CAB, calc-alkalic basalt; OFB, ocean floor basalt. The Nulato samples plot in the "within-plate basalt" field and the combined field for LKT, CAB, and OFB. Fields are from Pearce and Cann (1973).

15). Similar patterns are reported by Pallister and others (1989) in basaltic rocks in the Angayucham terrane bordering the north side of the Yukon-Koyukuk basin (fig. 2). Basaltic rocks tentatively assigned to the Angayucham(?) terrane in the adjoining Unalakleet quadrangle, however, have distinctive flat to LREE-depleted REE patterns (Patton and Moll-Stalcup, 1996). The range in major-element variation for samples of basaltic rocks from the Angayucham terrane bordering the north side of the Yukon-Koyukuk basin spans the range of data for the Nulato samples, but both suites appear highly altered (fig. 16).

Basalt and diabase samples from map unit TrMb in the Nulato quadrangle have variable patterns on trace-element plots (fig. 15). Analytical data for samples 82Pa1, 82Pa253, and a partial data set for sample ADGGS2461 show positive Nb and Ta anomalies, similar to oceanic island basalts. Data for samples 82Pa248, 82Pa249, and a partial data set for sample ADGGS2412 show Nb and Ta concentrations that are about the same as their alkalis and LREE contents. Sample 82Pa2 has a small negative Nb-Ta anomaly relative to LREE; and sample 82Pa242 has a stair-stepped pattern that steps down from alkalis to Nb-Ta to LREE. All of the samples are variably altered and as a result alkali element contents for some of them may not accurately reflect the original composition. Nb, Ta, and the LREE contents, however, are more immobile during alteration and therefore more reliable. Only one sample appears to have a small negative Nb and Ta anomaly relative to the LREE on plots; all other samples have either a positive Nb-Ta anomaly or a flat pattern.

Positive Nb-Ta anomalies are common in oceanic island basalts such as Hawaiian basalts or Bering Sea basalts (Moll-Stalcup, 1995). Flat patterns on plots are typical of mid-ocean ridge basalt or ocean island basalt. On a Pearce and Cann (1973) diagram that uses immobile elements to distinguish tectonic environment, most of the Nulato samples plot in the field for "within-plate basalt" or in an ambiguous field that includes "low-K tholeiite, calc-alkalic basalt, or ocean-floor basalt" (fig. 17). Be-

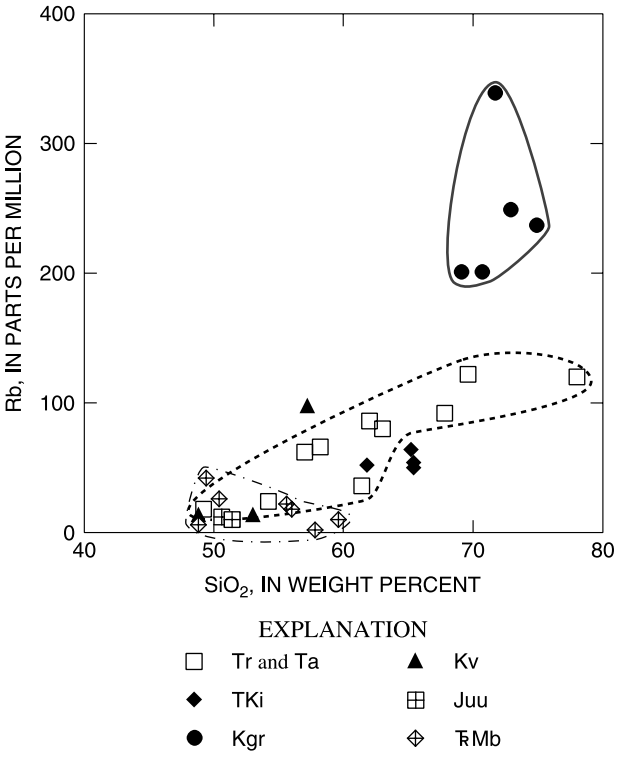

Figure 18. Plot of rubidium (Rb) compared with SiO_2 for rock samples from the Nulato quadrangle, west-central Alaska. Outlined areas show general range of compositions for map units Tr and Ta, Kgr, and TrMb. See Description of Map Units for explanation of map unit symbols.

cause the basalts of map unit TrMb lack strong Nb and Ta depletions relative to the LREE or the alkali elements, they are clearly not volcanic-arc basalts.

DISTINGUISHING GEOCHEMICAL CHARACTERISTICS OF MAP UNITS

• The Cretaceous granitic rocks of map unit Kgr can be distinguished from all the other map units by their very high Rb content (fig. 18). They also have lower Sr content than the early Tertiary and Late Cretaceous shallow intrusive rocks of unit TKi (fig. 19).

• The ultramafic-mafic complexes of map unit Juu, which are believed to form the underpinnings of the Koyukuk volcanic-arc terrane, have a lower TiO_2 content than basalt and diabase from map unit TrMb of the Angayucham-Tozitna oceanic terrane (fig. 20). The mafic rocks in map units Juu and TrMb both have high MgO contents (fig. 21) and low Rb (fig. 18) contents, as expected for rocks of basaltic composition. Although there is some overlap samples from map unit Juu have higher Sr contents than samples from map unit TrMb (fig. 19).

• Map units Tr, Ta, and TKi, which form a coherent suite of early Tertiary and Late Cretaceous continental volcanic-arc rocks, have a wider range of SiO_2 content than any of the other volcanic or intrusive map units in the Nulato quadrangle. However, individual samples of these early Tertiary and Late Cretaceous map units are not easily distinguished geochemically from samples of the Early Cretaceous volcanic arc rocks of map unit Kv.

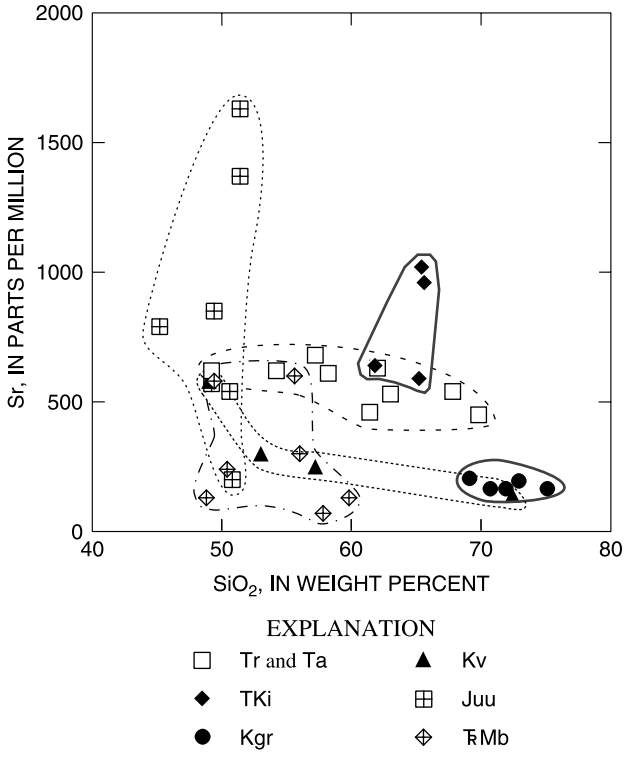

Figure 19. Plot of strontium (Sr) compared with SiO_2 for rock samples from the Nulato quadrangle, west-central Alaska. Outlined areas show general range of compositions for each map unit. See Description of Map Units for explanation of map unit symbols.

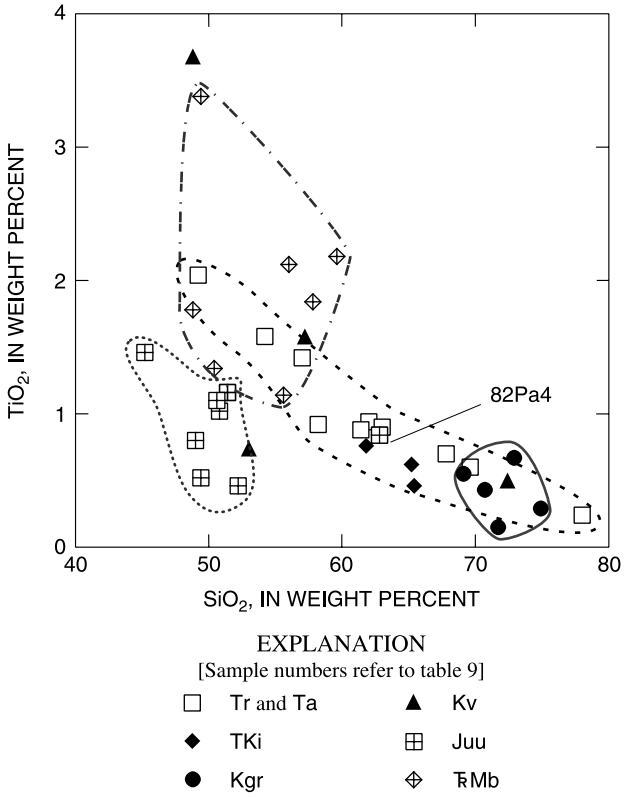

Figure 20. Plot of TiO_2 compared with SiO_2 for rock samples from the Nulato quadrangle, west-central Alaska. Outlined areas show general range of compositions for map units Tr and Ta, Kgr, Juu, and TrMb. Map unit Juu has lower TiO_2 than TrMb as expected in an arc-related suite. Sample 82Pa4 is of uncertain affinities and is discussed in the text. Data for map unit Kgr cluster tightly. The Late Cretaceous and early Tertiary volcanic rocks (Tr, Ta, and TKi) show decreasing TiO_2 with increasing SiO_2. See Description of Map Units for explanation of map unit symbols.

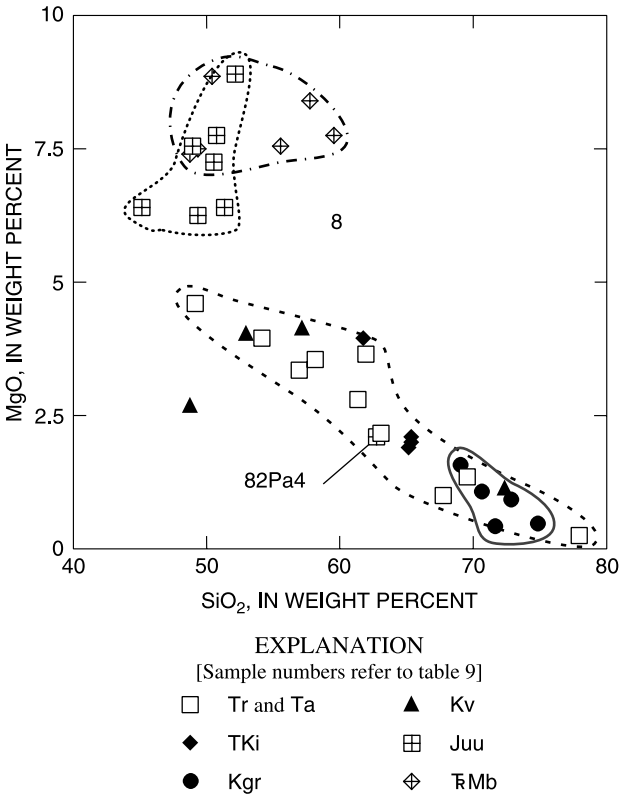

Figure 21. Plot of MgO compared with SiO_2 for rock samples from the Nulato quadrangle, west-central Alaska. Outlined areas show general range of compositions for map units Tr and Ta, Kgr, Juu, and TrMb. Sample 82Pa4 is not included in the field for Juu. As discussed in the text, it is of anomalous composition and uncertain affinities. See Description of Map Units for explanation of map unit symbols.

ACKNOWLEDGMENTS

Field data for the compilation of the geologic map were collected at intervals between 1954 and 1985 by W.W. Patton, Jr., 1954–1985; E.J. Moll-Stalcup, 1979–1981; R.S. Bickel, 1954–1956; J.M. Hoare, 1958; Bond Taber, 1958; A.R. Tagg, 1960; R.M. Chapman, 1974–1975; Christine Carlson, 1982; and S.E. Box, 1985. North Pacific Mining Corporation kindly provided copies of unpublished geologic field maps for parts of the Kaiyuh Mountains compiled by Anaconda Minerals Company between 1981 and 1985. Sarah Roeske generously shared the preliminary results of her 1994–1997 petrologic study of the metamorphic rocks of the Ruby terrane in the Kaiyuh Mountains. The map and pamphlet benefited from the technical reviews of W.P. Brosgé and R.A. Loney.

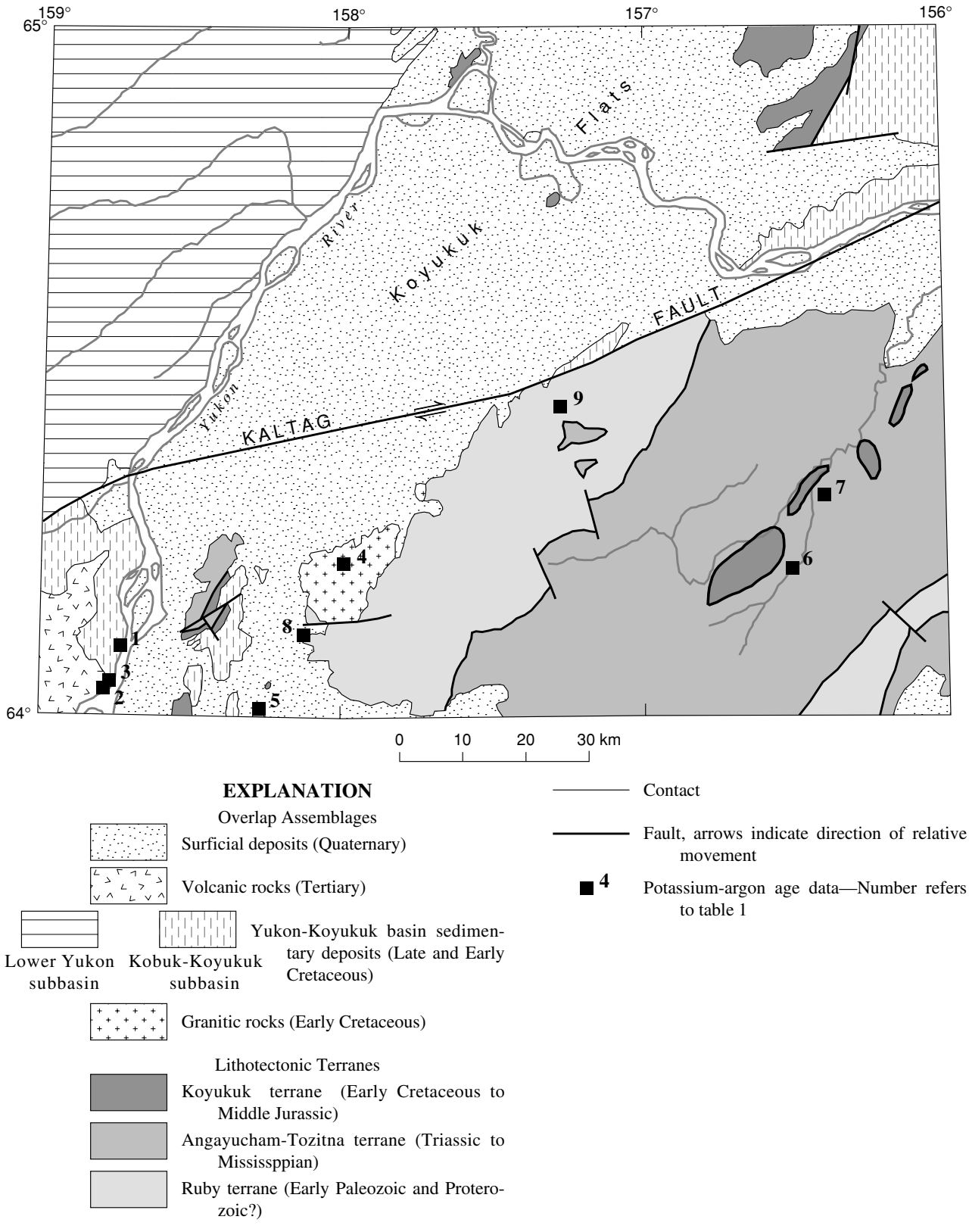

Figure 22. Generalized geologic map of the Nulato quadrangle showing the location of potassium-argon age samples listed in table 1.

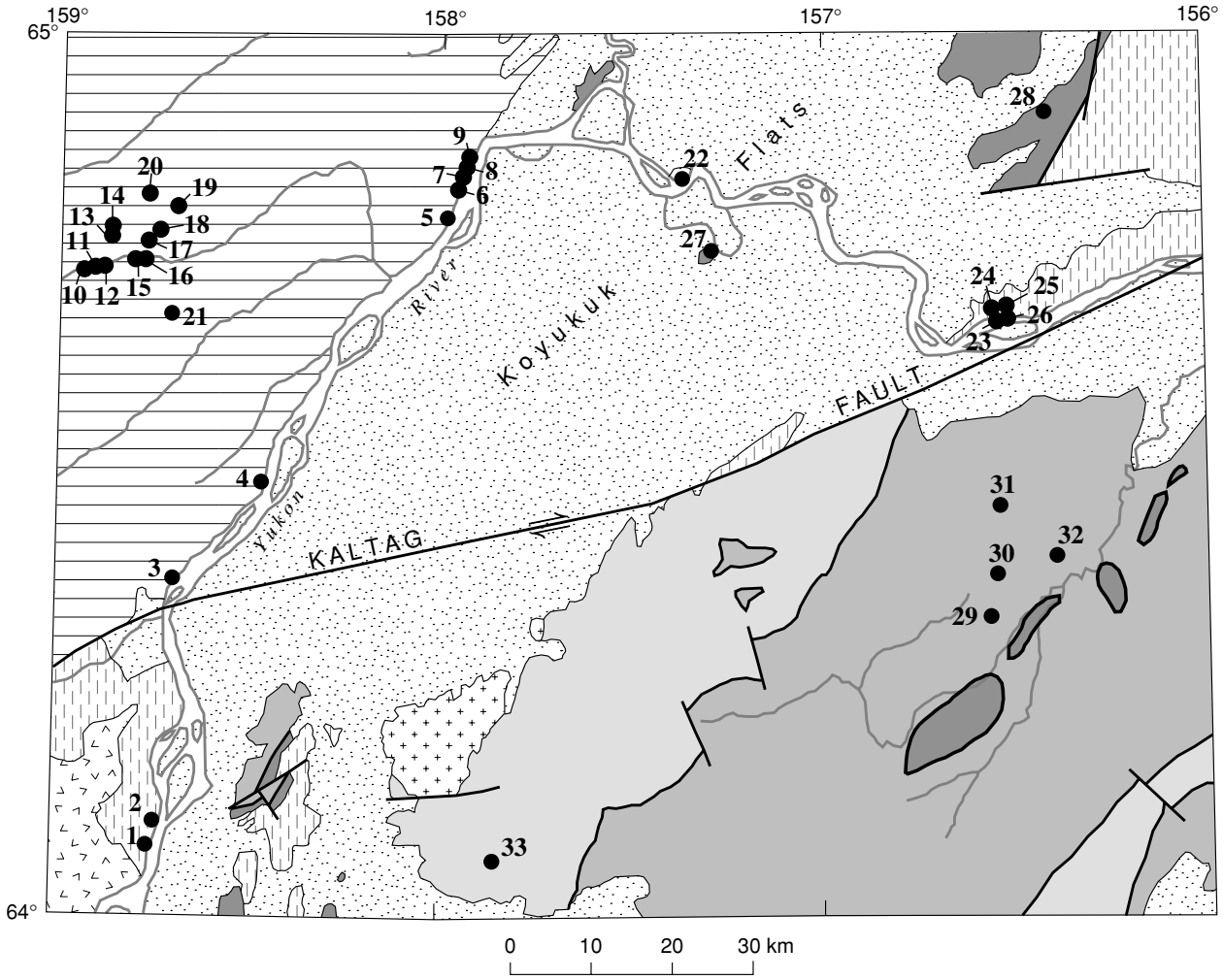

EXPLANATION

Overlap Assemblages

Surficial deposits (Quaternary)

Volcanic rocks (Tertiary)

Lower Yukon subbasin

Kobuk-Koyukuk subbasin

Yukon-Koyukuk basin sedimentary deposits (Late and Early Cretaceous)

Granitic rocks (Early Cretaceous)

Lithotectonic Terranes

Koyukuk terrane (Early Cretaceous to Middle Jurassic)

Angayucham-Tozitna terrane (Triassic to Mississppian)

Ruby terrane (Early Paleozoic and Proterozoic?)

Contact

Fault, arrows indicate direction of relative movement

33 Fossil locality—Number refers to table 2

Figure 23. Generalized geologic map of the Nulato quadrangle showing the location of fossil collections listed in table 2.

REFERENCES

Arth, J.G., Zmuda, C. C., Foley, N.K., Criss, R.E., Patton, W.W., Jr., and Miller, T.P., 1989, Isotopic and trace element variations in the Ruby batholith, Alaska, and the nature of the deep crust beneath the Ruby and Angayucham terranes: Journal of Geophysical Research, v. 94, no. B11, p. 15,941–15,955.

Aruscavage, P.J., and Crock, J.G., 1987, Atomic absorption methods, *in* Baedecker, P.A., ed., Methods for geochemical analyses: U.S. Geological Survey Bulletin 1770–C, p. C1–C6.

Baedecker, P.A., 1987, Methods for geochemical analyses: U.S. Geological Survey Bulletin 1770, 132 p.

Barnes, D.F., Mariano, John, Morin, R.L., Roberts, C.W., and Jachens, R.C., 1994, Incomplete isostatic gravity map of Alaska, *in* Plafker, G., and Berg, H.C., eds., The geology of Alaska, v. G–1 *of* The geology of North America: Boulder, Colo., Geological Society of America, plate 9, scale 1:250,000.

Barnes, F.F., 1967, Coal resources in Alaska: U.S. Geological Survey Bulletin 1242–B, p. B1–B36.

Bickel, R.S., and Patton, W.W., Jr., 1957, Preliminary geologic map of the Nulato and Kateel Rivers area, Alaska: U.S. Geological Survey Miscellaneous Geologic Investigations Map I–249, scale 1:125,000.

Box, S.E., and Patton, W.W., Jr., 1989, Igneous history of the Koyukuk terrane, western Alaska; Constraints on the origin, evolution, and ultimate collision of an accreted island-arc terrane: Journal of Geophysical Research, v. 94, no. B11, p. 15,843–15,867.

Box, S.E., Patton, W.W., Jr., and Carlson, Christine, 1985, Early Cretaceous evolution of the northeastern Yukon-Koyukuk basin, west-central Alaska, *in* The United States Geological Survey in Alaska—Accomplishments during 1984: U.S. Geological Survey Circular 967, p. 21–24.

Dempsey, W.J., Meuschke, J.L., and Andreasen, G.E., 1957, Total intensity aeromagnetic profiles of Koyukuk, Alaska: U.S. Geological Survey Open-File Report, 2 sheets.

Elder, W.P., and Miller, J.W., 1991, Maps showing fossil localities and checklists of Jurassic and Cretaceous macrofauna of western Alaska: U.S. Geological Survey Open File Report OF 91–629, 71 p., 3 plates.

Gill, J., 1981, Orogenic andesites and plate tectonics: New York, Springer-Verlag, 390 p.

Harris, R.A., Stone, D.B., and Turner, D.L., 1987, Tectonic implications of paleomagnetic and geochronologic data from the Yukon-Koyukuk province, Alaska: Geological Society of America Bulletin, v. 99, p. 362–375.

Hoare, J.M., Condon, W.H., and Patton, W.W., Jr., 1964, Occurrence and origin of laumontite in Cretaceous sedimentary rocks in western Alaska: U.S. Geological Survey Professional Paper 501–C, p. C74–C78.

Lichte, F.E., Golightly, D.W., and Lamothe, P.J., 1987, Inductively coupled plasma-atomic emission spectrometry, *in* Baedecker, P.A., ed., Methods for geochemical analyses: U.S. Geological Survey Bulletin 1770–B, p. B1–B10.

Loney, R.A., and Himmelberg, G.R., 1984, Preliminary report on the ophiolites in the Yuki River and Mount Hurst areas, west-central Alaska, *in* Coonrad, W.L., and Elliott, R.L., eds., The United States Geological Survey in Alaska—Accomplishments during 1981: U.S. Geological Survey Circular 868, p. 27–30.

Mertie, J.B., Jr., and Harrington, G.L., 1924, The Ruby-Kuskokwim region, Alaska: U.S. Geological Survey Bulletin 754, 129 p.

Miller, T.P., 1989, Contrasting plutonic rock suites of the Yukon-Koyukuk basin and the Ruby geanticline, Alaska: Journal of Geophysical Research, v. 94, no. B11, p. 15,969–15,988.

Mobil Exploration and Production Services, 1981, Nulato No. 1 test well: Alaska State Geological and Geophysical Surveys Geologic Material Center Report 15.

Moll-Stalcup, E.J., 1994, Latest Cretaceous and Cenozoic magmatism in mainland Alaska, *in* Plafker, G., and Berg, H.C., eds. The geology of Alaska, v. G–1 *of* The geology of North America: Boulder, Colo., Geological Society of America, p. 589–619.

———1995, The origin of the Bering Sea basalt province, western Alaska: Tikhookeanskaia Geologiia (Pacific Geology), v. 14, no. 4, p. 60–70.

Moll-Stalcup, Elizabeth, and Arth, J.G., 1989, The nature of the crust in the Yukon-Koyukuk province as inferred from the chemical and isotopic composition of five Late Cretaceous to early Tertiary volcanic fields in western Alaska: Journal of Geophysical Research, v. 94, no. B11, p.15,989–16,020.

Moll-Stalcup, E.J., and Patton, W.W., Jr., 1992, Geologic map of the Blackburn Hills volcanic field, western Alaska: U.S. Geological Survey Miscellaneous Field Studies Map MF–2199, scale 1:63,360.

Nilsen, T.H., 1989, Stratigraphy and sedimentology of the mid-Cretaceous deposits of the Yukon-Koyukuk basin, west-central Alaska: Journal of

Geophysical Research, v. 94, no. B11, p. 15,925–15,940.

Norton, D.R., and Papp, C.S., 1990, Determination of moisture and total water in silicate rocks, *in* Arbogast, G.F., Quality assurance manual for the Branch of Geochemistry: U.S. Geological Survey Open-File Report 90–668, p. 73–82.

Pallister, J.S., Budahn, J.R., and Murchey, B.L., 1989, Pillow basalts of the Angayucham terrane; oceanic plateau and island crust accreted to the Brooks Range: Journal of Geophysical Research, v. 94, no. B11, p. 15,901–15,924.

Papp, C.S.E., Aruscavage, P., and Brandt, E., 1990, Determination of ferrous oxides in geologic materials by potentiometric titration, *in* Arbogast, G.F., Quality assurance manual for the Branch of Geochemistry: U.S. Geological Survey Open-File Report 90–668, p. 139–145.

Patton, W.W., Jr., 1966, Regional geology of Kateel River quadrangle, Alaska: U.S. Geological Survey Miscellaneous Geologic Investigations Map I–437, scale 1:250,000.

———1992, Ophiolitic terrane bordering the Yukon-Koyukuk basin, Alaska: U.S. Geological Survey Open-File Report 92–20F, 7 p., 1 plate.

———1993, Ophiolitic terranes of northern and central Alaska and their correlatives in Canada and northeastern Russia: Geological Society of America Abstracts with Programs, v. 25, no. 5, p. 132.

Patton, W.W., Jr., and Bickel, R.S., 1956, Geologic map and structure sections along part of the lower Yukon River, Alaska: U.S. Geological Survey Miscellaneous Geologic Investigations Map I–197, scale 1:200,000.

Patton, W.W., Jr., and Box, S.E., 1989, Tectonic setting of the Yukon-Koyukuk basin and its borderlands: Journal of Geophysical Research v. 94, no. B11, p. 15,807–15820.

Patton, W.W., Jr., Box S.E., Moll-Stalcup, E.J., and Miller, T.P., 1994, Geology of west-central Alaska, *in* Plafker, G., and Berg, H.C., eds., The geology of Alaska, v. G–1 *of* The geology of North America: Boulder, Colo., Geological Society of America, p. 241–269.

Patton, W.W., Jr., and Hoare, J.M., 1968, The Kaltag fault, west-central Alaska: U.S. Geological Survey Professional Paper 600–D, p. D147–D153.

Patton, W.W., Jr., Miller, T.P., Chapman, R.M., and Yeend, Warren, 1978, Geologic map of the Melozitna quadrangle, Alaska: U.S. Geological Survey Miscellaneous Investigations Series Map I–1071, scale 1: 250,000.

Patton, W.W., Jr., and Moll-Stalcup, E.J., 1996, Geologic map of the Unalakleet quadrangle, west-central Alaska: U.S. Geological Survey Miscellaneous Investigations Series Map I–2559, scale 1:250,000.

Patton, W.W., Jr., Moll, E.J., Lanphere, M.A., and Jones, D.L., 1984, New age data for the Kaiyuh Mountains, west-central Alaska, *in* Coonrad, W. L., and Elliott, R.L., eds., The United States Geological Survey in Alaska—Accomplishments during 1981: U.S. Geological Survey Circular 868, p. 30–32.

Patton, W.W., Jr., and Tailleur, I.L., 1977, Evidence in the Bering Strait region for differential movement between North America and Eurasia: Geological Society of America Bulletin, v. 88, p. 1298–1304.

Pearce, J.A., and Cann, J.R., 1973, Tectonic setting of basic volcanic rocks determined using trace element analysis: Earth Planetary Science Letters, v. 19, p. 290–300.

Roeske, S.M., and McClelland, W.C., 1997, Preservation of the subduction zone boundary between the Ruby and Tozitna terrane, west-central Alaska: Geological Society of America Abstracts with Program, v. 29, no. 5, p. 60.

Solie, D.N., Bundtzen, T.K., Bowman, N.D., and Cruse, G.R., 1993a, Land selection unit 18 (Melozitna, Ruby, Nulato, and Kateel River quadrangles)—References, DGGS sample locations, geochemical, and major oxide data: Alaska Division of Geological and Geophysical Surveys Public Data File 93–18, 20 p.

Solie, D.N., Harris, E.E., Bundtzen, T.K., Wiltse, M.A., Newberry, R.J., Kline, J.T., and Smith, T.E., 1993b, Land selection unit 16 (Selawik, Candle, Norton Bay, Unalakleet, Kateel River, and Nulato quadrangles)—References, DGGS sample locations, geochemical and major oxide data: Alaska Division of Geological and Geophysical Surveys Public Data File 93–16, 54 p.

Solie, D.N., Wiltse, M.A., Gilbert, W.G., and Kline, J.T., 1993c, Land selection unit 17 (Nulato quadrangle)—References, DGGS sample locations, geochemical, and major oxide data: Alaska Division of Geological and Geophysical Surveys Public Data File 93–17, 15 p.

Streckeisen, A., 1979, Classification and nomenclature of volcanic rocks, lamprophyres, carbonatites, and melitic rocks—Recommendations and suggestions of the IUGS Subcommission of the Systematics of Igneous Rocks: Geology, v. 7, p. 331–335.

Taggart, J.E., Jr., Bartel, A., and Siems, D.F., 1990, High precision major element analyses of rocks and minerals by wavelength dispersive X-ray fluorescence spectroscopy, *in* Arbogast, G.F.,

Quality assurance manual for the Branch of Geochemistry: U.S. Geological Survey Open-File Report 90–668, p. 166–172.

Thompson, R.N., Morrison, M.A., Hendry, G.L., and Parry, S.J., 1984, An assessment of the relative roles of crust and mantle in magma genesis—An elemental approach: Royal Society of London Philisophical Transactions A, v. 310, p. 549–590.

Wahrhaftig, C., Bartsch-Winkler, S., and Stricker, G.D., 1994, Coal in Alaska, *in* Plafker, G., and Berg, H.C., eds., The geology of Alaska, v. G–1 of The geology of North America: Boulder, Colo., Geological Society of America, p. 937–978.

Wheately, M.R., and Rock, N.M.S., 1988, Spider—A Macintosh program to generate normalized multi-element "spidergrams" (version 3.01): American Mineralogist, v. 73, p. 919–921.

Wilson, S.A., Kane, J.S., Crock, J.G., and Hatfield, D.B., 1987, Chemical methods of separation for optical emission, atomic absorption spectromtry, and colorimetry, *in* Baedecker, P.A., Methods for geochemical analysis: U.S. Geological Survey Bulletin 1770, p. D1–D14.

Zietz, Isidore, Patton, W.W., Jr, and Dempsey, W.J., 1959, Preliminary interpretation of total-intensity aeromagnetic profiles of the Koyukuk area, Alaska: U.S. Geological Survey Open-File Report 59–132, 7 p.

Table 1. *Potassium-argon ages for samples from Nulato quadrangle, west-central Alaska*

Fig. 1 No.	Latitude Longitude	Field No.	Map unit	Rock type	Mineral or whole rock analyzed	Age (millions of years)	Reference
1	64°05.4'N 158°43.6'W	DT 83-13D DT 83-13A DT 83-13B	Ta	basalt	whole rock whole rock whole rock	52.4±1.6 53.7±1.6 56.5±1.7	Harris and others, 1987
2	64°02.7'N 158°45.2'W	DT 83-15A	Tr	dacite	hornblende biotite	49.1±1.5 53.3±1.6	Harris and others, 1987
3	64°02.8'N 158°45.2'W	81APa319	Tr	dacite	hornblende biotite	47.6±1.4 50.6±1.5	Moll-Stalcup and Arth, 1989
4	64°13.6'N 157°55.9'W	79APa548	Kgr	granite	biotite	112±3.4	Patton and others, 1984
5	64°00.0'N 158°16.6'W	79APa552A	Juu	gabbro pegmatite	hornblende	151±4.5	Patton and others, 1984
6	64°12.0'N 156°30.5'W	79APa525A	Juu	garnet amphibolite	hornblende	172±5.2	Patton and others, 1984
7	64°18.4'N 156°23.3'W	79APa521C	Juu	gabbro pegmatite	hornblende	269±8	Patton and others, 1984
8	64°07.7'N 158°05.8'W	79APa551	PzPs	muscovite schist	muscovite	134±4.0	Patton and others, 1984
9	64°26.9'N 157°17.8'W	79APa526	PzPs	quartz mica schist	muscovite	136±4.1	Patton and others, 1984

Table 2. *Fossil collections from the Nulato quadrangle, west-central Alaska*

CRETACEOUS

Fig. 2 No.	Latitude	Longitude	Field No.	Mesozoic locality	Fossils (identifications by Elder and Miller, 1991)	Map unit	Age
1	64°04.4'N	158°44.2'W	56APa163	26245	*Arctica*? sp.	Ks	Cretaceous?
2	64°04.6'N	158°43.9'W	56APa155	26244	*Yaadia whiteavesi* (Packard)	Ks	M. Albian
3	64°22.5'N	158°40.2'W	54APa242	25306	*Inoceramus altifluminis* McLearn	Ksm	M. Albian
			07Atkin34	4793	*Arctica?* sp., Inoceramid indet., *Lucina* sp., Ostreaid, *Pleuromya* sp.	Ksm	Cretaceous?
4	64°27.9'N	158°28.1'W	54APa240	25305	*Cardium* sp., Mytilid, *Inoceramus altifluminis* McLearn, *Yaadia whiteavesi* (Packard)	Ksm	M Albian
			03AH25a	2931	*Arctica* sp., Gastropod indet.,	Ksm	Cretaceous?
5	64°46.6'N	157°59.0'W	85SB210A	M8333	*Arctica*? sp.	Ksm	Cretaceous?
			85SB210B	M8334	*Cardium* sp., *Yaadia* sp.	Ksm	Cretaceous
6	64°49.1'N	157°57.3'W	54APa209	25300	*Arctica*? sp., *Cardium* sp., *Inoceramus altifluminis* McLearn, *Panopea*? sp., *Psilomya* sp., *Yaadia whiteavesi* (Packard), *Acteonella*? sp.	Ksm	M. Albian
7	64°49.5'N	157°56.8'W	54APa207	25299	*Arctica*? sp., *Cardium* sp., *Panopea*? sp., *Pholadomya* sp., *Protocardia* sp., *Solecurtus*? sp.	Ksm	Cretaceous?
8	64°49.9'N	157°56.2'W	54APa206	25298	*Cardium* sp., *Pholadomya* sp., *Protocardia* sp., *Psilomya*? sp.	Ksm	Cretaceous?
9	64°50.5'N	157°55.5'W	02AC250	2677	Inoceramid indet., *Panopea*? sp., *Thracia* sp.	Ksm	Cretaceous?
			02AC244	2678	*cf. Yaadia whiteavesi* (Packard), *Gastroplites* sp.	Ksm	M. Albian
			02AC249	2679	Mytilid, Ostreaid	Ksm	Cretaceous?
			02AC251	2680	*Arctica*? sp., *Cardium* sp., *Pholadomya* sp., Tellinid	Ksm	Cretaceous?
			54APa204	25297	*Cardium* sp., *Cucullaea*? sp.	Ksm	Cretaceous?
			85ASB207	M8331	*cf. Inoceramus altifluminis* McLearn, *Panopea*? sp. *Solecturus*? sp.	Ksm	M. Albian
10	64°43.0'N	158°56.4'W	55ABL162	25888	*Lopatinia dowlingi* (McLearn), Mytilid, *Tancredia* sp.	Ksm	Cretaceous?
			85APa72	M8335	*Arctica?* sp.	Ksm	Cretaceous?
11	64°43.1'N	158°55.3'W	55ABL160	25887	*Inoceramus altifluminis* McLearn	Ksm	M. Albian
12	64°43.0'N	158°54.6W	55ABL157	25886	*Arctica*? sp., *Cardium* sp., Mytilid	Ksm	Cretaceous?
13	64°45.7'N	158°52.2'W	55ABL178	25890	*Anomia* sp., *Cardium* sp., Ostreaid	Ksm	Cretaceous?
14	64°45.9'N	158°52.2'W	55ABL179	25891	*Lopatinia dowlingi* (McLearn)	Ksm	Cretaceous?
15	64°43.6'N	158°50.2W	55ABL152	25884	*Cardium* sp., *Lucina* sp., Mytilid, *Yaadia whiteavesi* (Packard)	Ksm	M. Albian
16	64°43.8'N	158°49.4'W	55ABL154	25885	*Arctica*? sp., *Cardium* sp., Mytilid, Ostreaid, *Pleuromya* sp., *Yaadia whiteavesi* (Packard)	Ksm	M. Albian
17	64°44.1'N	158°49.0'W	55ABL183	25892	Inoceramid indet., *Pleuromya* sp.	Ksm	Cretaceous?
18	64°44.5'N	158°48.4'W	55ABL184	25893	Mytilid	Ks	Cretaceous?
19	64°46.5'N	158°44.8'W	55ABL185	25894	Mytilid	Ks	Cretaceous?
20	64°48.1'N	158°46.6'W	55ABL187	25895	*Entolium* sp., *Tancredia* sp.	Ksm	Cretaceous?
21	64°40.0'N	158°43.1'W	55ABL169	25889	Mytilid	Ks	Cretaceous?
22	64°49.4'N	157°21.6'W	03AH17	2926	*Arctica*? sp., *Lucina* sp., *Thracia* sp.	Ksm	Cretaceous?
			54APa189	25294	*Arctica*? sp., *Panopea*? sp., *Psilomya* sp., *Gastroplites* sp., *Anchura*? sp.	Ksm	M Albian
			03AH17A	2927	*cf. Yaadia whiteavesi* (Packard), *Gastroplites* sp.	Ksm	M. Albian
			85SB202B	M8329	*Paragastroplites flexicostatus* Imlay	Ksm	M. Albian
			85SB203B	M8330	*Panopea* sp., *Pleuromya* sp.	Ksm	M. Albian
23	64°39.9'N	156°31.8'W	03AH15	2924	*Arctica*? sp., *Lucina* sp.	Ks	Cretaceous?
			54APa174	25291	*Arctica*? sp.	Ks	Cretaceous?
			54APa178	25292	*Arctica*? sp., *Solecurtus*? sp.	Ks	Cretaceous?
			85SB202	M8328	Inoceramid indet., Ostreaid	Ks	Cretaceous?
24	64° 40.0'N	156°32.6'W	54APa180	25293	*Inoceramus altifluminis* McLearn	Ks	M. Albian
25	64°41.2'N	156°31.4'W	ST241	M7376	*Yaadia californiania* (Packard), Ammonite indet.	Ks	M. Albian
26	64°40.0'N	156°31.0'W	54APa168	25290	*Arctica*? sp., *Panopea*? sp., *Yaadia whiteavesi* (Packard)	Ks	M. Albian
27	64°45.3'N	157°18.2'W	C7	21417	*Buchia sublaevis* (Pavlow)	Kv	Valanginian
28	64°54.9'N	156°22.0'W	60APa27	M1054	*Buchia crassicolis solida* (Lahusen)	Kv	Valanginian

EARLY MESOZOIC AND PALEOZOIC

Fig. 2 No.	Latitude	Longitude	Field No.	Fossils	Map unit	Age	Reference
29	64°18.8'N	156°36.5'W	79APa510	radiolaria	TrMb	Carboniferous	Patton and others, 1984
30	64°22.1'N	156°33.7'W	79APa513A	radiolaria	TrMb	Carboniferous	Patton and others, 1984
31	64°28.6'N	156°32.7'W	79APa516	radiolaria	TrMb	Carboniferous	Patton and others, 1984
32	64°24.0'N	156°25.6'W	79APa518A	radiolaria	TrMb	Triassic	Patton and others, 1984
33	64°04.3'N	157°52.4'W	Illinois Cr., drillholes WP-84-11,16	conodonts	PzC	Ordovician	A.G. Harris, written commun, 1984

Table 3. *Major oxide and trace-element composition of early Tertiary rhyolite and dacite from map unit Tr from the Nulato quadrangle, west-central Alaska*

[Major elements in weight percent; trace elements in parts per million. All major oxides except FeO, CO_2, H_2O+, and H_2O- by X-ray fluorescence following methods of Taggart and others (1990). FeO by titration following method of Papp and others (1990). FeO values in italics calculated assuming $Fe_2O_3/FeO = 0.3$. CO_2 and H_2O by methods of Norton and Papp (1990). Trace elements by instrumental neutron activation analysis (INAA) unless otherwise noted in first column by XRF, energy-dispersive X-ray fluorescence; ICP, inductively coupled plasma-emission spectrometry; HGA, heated graphite atomizer-atomic absorption spectrometry (Aruscavage and Crock, 1987); SIE, selected-ion electrode; or ICP-AES, inductively coupled plasma-atomic emission spectrometry (Lichte and others, 1987). LOI, loss on ignition. Methods described in Baedecker (1987). <, less than; nd, not accurately determined (analytical precision greater than 15%); --, not analyzed. All analyses by USGS; Reston, Va. and Lakewood, Colo.]

Sample No.	81Pa319	82Pa76	79Pa519
Rock type	Dacite	Rhyolite	Dacite
Fig. 5 No.	1	2	3
Latitude	64°02.8'	64°05.7'	64°20.1'
Longitude	158°45.2'	158°58.2'	156°17.4'
SiO_2	66.3	76.3	66.3
Al_2O_3	14.3	12.1	16.7
Fe_2O_3	2.74	0.38	0.46
FeO	0.72	0.19	*1.58*
MgO	1.27	0.21	0.95
CaO	2.77	0.75	4.22
Na_2O	2.88	3.26	3.60
K_2O	3.37	4.43	3.07
TiO_2	0.57	0.22	0.68
P_2O_5	0.18	<.05	0.28
MnO	0.08	<.02	0.04
LOI	4.40	0.87	1.07
H_2O+	1.80	0.43	- -
H_2O-	2.00	0.31	- -
CO_2	0.02	<.01	- -
Total	99.00	98.58	98.95
Rb	111	119	91.09
Rb (XRF)	121	- -	- -
Cs	3.59	5.23	1.85
Sr	- -	- -	539.20
Sr (XRF)	441	- -	- -
Ba	1290	1350	1715
Ba (XRF)	1230	- -	- -
La	41	45.5	52.42
Ce	72.8	71.2	87.75
Nd	30	22	31.89
Sm	5.46	3.48	6.32
Eu	1.2	0.607	1.31
Gd	4.5	3.5	- -
Tb	0.688	0.424	0.69
Tm	0.29	0.39	- -
Yb	2.82	1.57	1.96
Lu	0.427	0.261	0.28
Y (XRF)	26	- -	- -
Zr	230	170	210.80
Zr (XRF)	223	- -	- -
Hf	5.90	4.74	5.37
Nb (XRF)	17	- -	- -
Ta	1.55	1.49	1.12
Th	13.4	18.0	13.30
U	3.02	7.08	3.51
Co	5.77	0.63	6.31
Cr	6.2	nd	17.56
Ni	- -	- -	nd
Sc	7.35	1.99	9.87
Zn	53.1	19.0	73.03
Sb	0.24	1.4	0.16
F (SIE)	- -	0.03	- -
W (ICP-AES)	- -	<3.0	- -
Sn (HGA)	- -	1.4	- -

Table 4. *Major oxide and trace-element composition of early Tertiary andesite and basalt from map unit Ta from the Nulato quadrangle, west-central Alaska*

[Major elements in weight percent; trace elements in parts per million. All major oxides except FeO, CO_2, H_2O+, and H_2O- by X-ray fluorescence following methods of Taggart and others (1990). FeO by titration following method of Papp and others (1990). FeO values in italics calculated assuming $Fe_2O_3/FeO = 0.3$. CO_2 and H_2O by methods of Norton and Papp (1990). Trace elements by instrumental neutron activation analysis (INAA) unless otherwise noted in first column by XRF, energy-dispersive X-ray fluorescence. LOI, loss on ignition. Methods described in Baedecker (1987). <, less than; nd, not accurately determined (error greater than 15%); - -, not analyzed. USGS analyses made in Reston, Va., and Lakewood, Colo. Alaska Division of Geological and Geophysical Surveys (ADGGS) samples previously published in Solie and others (1993b)]

Sample No.	81Pa321	81Pa323	81Pa326	91Bt422	91Bt427	81Pa335	79Pa523a
Analyses by	USGS	USGS	USGS	ADGGS	ADGGS	USGS	USGS
Rock type	Andesite	Andesite	Basalt	Andesite	Andesite	Basalt	Andesite
Fig. 5 No.	4	5	6	7	8	9	10
Latitude	64°01.2'	64°00.8'	64°00.2'	64°05.4'	64°04.9'	64°05.3'	64° 02.0'
Longitude	158°47.0'	158°48.4'	158°52.0'	158°56.8'	158°56.7'	158°43.6'	156° 13.8'
SiO_2	55.7	60.6	48.0	57.1	61.6	51.5	60.6
Al_2O_3	15.9	16.7	16.7	17.8	16.7	16.5	15.8
Fe_2O_3	4.50	3.09	7.28	4.05	2.43	3.20	1.15
FeO	3.80	2.80	3.80	2.00	2.70	6.00	*3.96*
MgO	3.26	2.74	4.47	3.45	2.05	3.71	3.56
CaO	6.86	6.22	10.80	7.45	5.36	7.65	5.46
Na_2O	3.57	3.60	3.22	3.37	3.96	3.43	3.26
K_2O	2.01	1.65	0.71	1.62	1.71	1.02	2.59
TiO_2	1.37	0.85	1.98	0.90	0.88	1.50	0.90
P_2O_5	0.46	0.28	0.49	0.21	0.37	0.40	0.35
MnO	0.17	0.10	0.15	0.11	0.13	0.15	0.09
LOI	2.56	1.62	2.65	1.62	2.00	3.74	1.19
H_2O+	0.36	0.5	1.00	- -	- -	2.42	- -
H_2O-	1.10	0.92	1.10	- -	- -	0.18	- -
CO_2	0.08	0.01	0.08	- -	- -	1.88	- -
Total	99.14	100.06	99.78	99.68	99.89	99.54	98.91
Rb	58	39	nd	- -	- -	25	85.01
Rb (XRF)	61	36	17	65	79	23	
Cs	3.04	0.45	nd	- -	- -	0.42	2.92
Sr	- -	- -	- -	- -	- -	- -	629.20
Sr(XRF)	678	454	616	602	521	617	- -
Ba	820	1030	440	- -	- -	681	1491
Ba (XRF)	841	1040	464	1030	1320	691	- -
La	34.6	40.0	23.8	- -	- -	33.7	49.66
Ce	65.7	67.7	49.7	- -	- -	62.9	85.93
Nd	30	29	29	- -	- -	31	32
Sm	6.22	5.39	6.31	- -	- -	6.31	6.58
Eu	1.59	1.35	1.79	- -	- -	1.72	1.43
Gd	5.5	4.1	5.7	- -	- -	5.8	- -
Tb	0.74	0.637	0.917	- -	- -	0.858	0.72
Tm	0.40	0.34	0.44	- -	- -	0.53	- -
Yb	2.43	2.43	2.99	- -	- -	2.88	2.28
Lu	0.353	0.382	0.433	- -	- -	0.443	0.32
Y (XRF)	23	24	27	<10	31	26	- -
Zr	160	180	nd	- -	- -	150	244
Zr (XRF)	166	204	154	165	232	186	- -
Hf	3.74	4.55	3.23	- -	- -	4.10	5.28
Nb (XRF)	17	12	15	21	27	10	- -
Ta	1.26	0.947	0.775	- -	- -	0.75	1.12
Th	7.39	5.65	1.40	- -	- -	4.97	10.97
U	2.21	1.50	0.10	- -	- -	0.87	2.70
Co	28.4	16.4	38.7	- -	- -	26.2	14.9
Cr	30.7	35.9	104	- -	- -	13.0	78.8
Cr (XRF)	- -	- -	- -	27	<10	- -	- -
Sc	17.8	14.6	32.4	- -	- -	23.6	12.9
Zn	73.2	71.4	101	- -	- -	90.1	67.2
Sb	0.33	<.5	<.6	- -	- -	0.33	0.15

Table 5. *Major oxide and trace-element composition of early Tertiary and Late Cretaceous shallow intrusive rocks from map unit TKi from the Nulato quadrangle, west-central Alaska*

[Major elements in weight percent; trace elements in parts per million. All major oxides by X-ray fluorescence following methods of Taggart and others (1990). FeO values in italics were calculated by assuming Fe_2O_3/FeO =0.3. Trace elements by instrumental neutron activation analysis (INAA) unless otherwise noted in first column by the acronym: XRF, energy-dispersive X-ray fluorescence. LOI, loss on ignition. Methods described in Baedecker (1987). <, less than; nd, not accurately determined (error greater than 15%); - -, not analyzed. USGS analysts: C.A. Palmer, Reston, Va.; D.F. Siems, J.S. Mee, Lakewood, Colo. Alaska Division of Geological and Geophysical Surveys (ADGGS) samples previously published in Solie and others (1993a)]

Sample No.	81Pa305-3	74Pa172a	ADGGS4206	ADGGS4017
Analyses by	USGS	USGS	ADGGS	ADGGS
Rock type	Andesite	Dacite	Monzonite?	Granodiorite
Fig. 5 No.	11	12	13	14
Latitude	64° 39.9'	64° 43.8'	64° 52.8'	64° 52.8'
Longitude	156° 31.8'	156° 25.1'	156° 11.4'	156° 10.4'
SiO_2	59.8	63.0	63.45	63.17
Al_2O_3	16.5	15.9	17.1	16.95
Fe_2O_3	1.08	0.98	3.15	3.06
FeO	*3.71*	*3.37*	0.68	0.90
MgO	3.78	1.81	2.01	1.9
CaO	5.38	4.95	4.26	4.39
Na_2O	4.06	3.40	4.48	4.33
K_2O	1.39	2.17	1.10	1.25
TiO_2	0.73	0.58	0.44	0.43
P_2O_5	0.19	0.34	0.17	0.21
MnO	0.08	0.07	0.04	0.05
LOI	2.52	2.20	1.86	2.37
Total	99.22	98.77	98.74	99.01
Rb	51.53	62.32	- -	- -
Rb (XRF)	- -	- -	54	50
Cs	2.81	0.95	- -	- -
Sr	639.90	580.40	- -	- -
Sr (XRF)	- -	- -	953	1013
Ba	1247.00	1327.00	- -	- -
Ba (XRF)	- -	- -	1400	1400
La	19.75	53.96	- -	- -
Ce	33.71	88.44	- -	- -
Nd	14.44	29.50	- -	- -
Sm	3.05	5.31	- -	- -
Eu	0.88	1.27	- -	- -
Tb	0.37	0.54	- -	- -
Yb	1.23	1.82	- -	- -
Lu	0.18	0.25	- -	- -
Y (XRF)	- -	- -	10	7
Zr (XRF)	- -	- -	119	107
Hf	2.61	4.37	- -	- -
Nb (XRF)	- -	- -	<5	28
Ta	0.48	0.97	- -	- -
Th	5.19	11.14	- -	- -
U	2.02	2.39	- -	- -
Co	18.46	10.60	- -	- -
Cr	73.67	16.04	- -	- -
Cr (XRF)	- -	- -	28	27
Sc	15.43	9.24	- -	- -
Zn	51.29	62.33	- -	- -
Sb	0.45	0.25	- -	- -

Table 6. *Major oxide and trace-element composition of Early Cretaceous granite from map unit Kgr from the Nulato quadrangle, west-central Alaska*

[Major elements in weight percent; trace elements in parts per million. Trace elements by instrumental neutron activation analysis (INAA) unless otherwise noted in first column by XRF, energy-dispersive X-ray fluorescence. LOI, loss on ignition. nd, not accurately determined (error greater than 15%); - -, not analyzed. For USGS samples, all major oxides by X-ray fluorescence following methods of Taggart and others (1990). FeO values in italics calculated by assuming Fe_2O_3/FeO =0.3. Trace element methods described in Baedecker (1987). USGS analysts: D.F. Siems, J.S. Mee, Lakewood, Colo.; C.A. Palmer, Reston, Va. Analyses by Alaska Division of Geological and Geophysical Surveys (ADGGS) were previously published in Solie and others (1993c)]

Sample No.	79Pa540	79Pa548	79Pa549	ADGGS2473
Analyses by	USGS	USGS	USGS	ADGGS
Rock type	Granite	Granite	Granite	Granite
Fig. 5 No.	15	16	17	18
Latitude	64°19.0'	64°13.6'	64°10.4'	64°19.1'
Longitude	157°45.2'	157°55.9'	157°56.8'	157°46.2'
SiO_2	72.1	69.6	68.0	74.6
Al_2O_3	12.9	14.8	14.6	13.0
Fe_2O_3	0.63	0.68	0.91	0.44
FeO	*2.17*	*2.34*	*3.15*	1.00
MgO	0.84	1.02	1.51	0.44
CaO	1.76	2.43	2.67	1.41
Na_2O	2.16	2.80	2.50	2.99
K_2O	5.33	4.10	4.26	5.09
TiO_2	0.65	0.40	0.52	0.265
P_2O_5	0.18	0.15	0.18	0.07
MnO	0.04	0.06	0.05	0.03
LOI	0.26	0.39	1.02	0.47
Total	99.02	98.77	99.37	99.81
Rb	247.00	199.30	199.00	- -
Rb (XRF)	- -	- -	- -	236
Cs	6.26	15.29	8.52	- -
Sr	184.20	158.20	196.50	- -
Sr (XRF)	- -	- -	- -	155
Ba	563.40	679.00	742.20	- -
Ba (XRF)	- -	- -	- -	525
La	24.88	35.59	48.77	- -
Ce	50.15	64.93	82.84	- -
Nd	23.08	24.31	36.57	- -
Sm	4.56	5.55	7.76	- -
Eu	0.86	0.98	1.14	- -
Tb	0.47	0.70	0.95	- -
Yb	1.42	2.34	3.44	- -
Lu	0.21	0.32	0.47	- -
Y (XRF)	- -	- -	- -	41
Zr	303.90	143.50	152.70	- -
Zr (XRF)	- -	- -	- -	197
Hf	8.03	4.09	5.01	- -
Nb (XRF)	- -	- -	- -	29
Ta	0.96	1.27	1.28	- -
Th	10.10	16.35	21.67	- -
U	2.49	3.32	3.61	- -
Co	5.86	6.90	11.48	- -
Cr	4.51	18.69	28.08	- -
Cr (XRF)	- -	- -	- -	14
Sc	4.30	8.03	11.89	- -
Zn	26.04	29.68	22.43	- -
As	nd	17.91	5.30	- -
Sb	nd	0.28	0.21	- -

Table 7. *Range of major oxide and trace-element composition of Early Cretaceous granite from map unit Kgr from the Khotol pluton in the Nulato quadrangle compared with two granite samples from the Melozitna pluton in the Melozitna quadrangle, west-central Alaska*

[Major elements in weight percent; trace elements in parts per million. Trace elements for Nulato samples given in table 6. Anayses of Melozitna pluton from Arth and others, 1989. Rb and Sr for Melozitna pluton analyzed by energy dispersive XRF; other element were analyzed by INAA.]

	Khotol pluton	Melozitna pluton	
Rock type	Granite	Granite	Granite
Sample No.	79Pa540, 548,549, ADGGS2473	AK683	AK682
Latitude	see table 6	65°21'	65°20'
Longitude	" "	154°05'	154°20'
SiO_2	68.0-74.6	71.6	73.2
Al_2O_3	12.9-14.8	13.5	14.1
Fe_2O_3	0.44-0.91	0.83	0.46
FeO	1.00-3.15	1.6	0.88
MgO	0.44-1.51	0.62	0.43
CaO	1.41-2.67	1.95	0.94
Na_2O	2.16-2.99	2.49	3.12
K_2O	4.10-5.33	5.30	4.85
TiO_2	0.265-0.65	0.37	0.17
P_2O_5	0.07-0.18	0.08	0.14
MnO	0.03-0.06	0.03	0.04
LOI	0.26-1.02	0.86	0.93
Total	98.8-99.8	99.20	99.10
Rb	199-247	269	552
Cs	6.26-15.29	5.82	13.7
Sr	155-184	237	29
Ba	525-742	660	134
La	25-49	105	45.2
Ce	50-83	200	99
Nd	23-37	72	44
Sm	4.6-7.8	12.2	9.13
Eu	0.9-1.1	1.06	0.22
Tb	0.5-1.0	1.1	1.11
Yb	1.4-3.4	3.05	4.78
Lu	0.2-0.5	0.451	0.679
Zr	144-304	244	90
Hf	4.1-8.0	6.55	5.07
Ta	1.0-1.3	1.3	3.64
Th	10.1-21.7	39.4	75
U	2.5-3.6	5.26	10.6
Co	5.9-11.5	4.06	0.481
Cr	4.5-28.1	12.5	5.4
Sc	4.3-11.9	5.85	0.78
Zn	22.4-29.7	34.3	1.1

Table 8. *Major oxide and trace-element composition of four samples of Early Cretaceous andesitic volcanic rocks from map unit Kv from the Nulato quadrangle, west-central Alaska*

[Major elements in weight percent; trace elements in parts per million. All major oxides except FeO, CO_2, H_2O+, and H_2O- by X-ray fluorescence following methods of Taggart and others (1990). FeO by titration following method of Papp and others (1990). CO_2 and H_2O by methods of Norton and Papp (1990). Trace elements by instrumental neutron activation analysis (INAA) unless otherwise noted in first column by XRF, energy-dispersive X-ray fluorescence. LOI, loss on ignition. Methods described in Baedecker (1987). <, less than; nd, not accurately determined (error greater than 15%); - -, not analyzed. USGS analyses done in Reston, Va., and Lakewood, Colo.]

Sample No.	82Pa3	81Pa340 duplicate	81Pa340	81Pa338a duplicate	81Pa338a	81Pa338c
Rock type	Basalt	Rhyolite tuff	Rhyolite tuff	Basalt	Basalt	Andesite
Fig. 5 No.	20	21	21	22	22	23
Latitude	64°11.6'	64°55.1'	64°55.1'	64°54.3'	64°54.3'	64°54.3'
Longitude	158°24.3'	157°37.8'	157°37.8'	157°38.5'	157°38.5'	157°38.5'
SiO_2	48.8	70.8		45.0		52.4
Al_2O_3	16.7	12.8		16.4		13.8
Fe_2O_3	3.05	3.03		5.59		1.78
FeO	5.18	2.00		6.50		6.14
MgO	3.70	1.12		2.46		3.77
CaO	10.60	1.12		6.46		5.92
Na_2O	2.69	6.05		4.80		2.02
K_2O	0.43	0.20		0.83		3.75
TiO_2	0.67	0.47		3.38		1.44
P_2O_5	0.09	0.15		0.42		0.33
MnO	0.20	0.11		0.25		0.18
LOI	7.54	1.52		6.40		6.78
H_2O+	2.66	1.10		3.30		- -
H_2O-	0.74	0.46		0.56		- -
CO_2	4.33	0.03		3.60		- -
Total	99.84	99.44		99.54		98.31
Rb	nd	<20	nd	<30	12.92	96.43
Rb (XRF)	14	<5	- -	13	- -	- -
Cs	nd	<0.4	nd	0.6	0.42	2.14
Sr	nd	- -	nd		621.60	248.30
Sr (XRF)	297	138	- -	572	- -	- -
Ba	nd	140	145.60	692	682.00	822.80
Ba (XRF)	220	151	- -	690	- -	- -
La	nd	30.7	32.06	16.5	16.55	21.36
Ce	nd	67.8	68.23	37.0	38.04	43.30
Nd	nd	45.1	41.19	27	23.16	23.32
Sm	nd	11.8	12.06	7.00	7.17	6.49
Eu	nd	3.06	3.06	2.29	2.28	1.80
Gd	nd	13.0	- -	7.7	- -	- -
Tb	nd	1.96	2.10	1.25	1.28	1.05
Tm	nd	1.20	- -	0.50	- -	- -
Yb	nd	8.44	8.24	3.88	3.88	4.06
Lu	nd	1.22	1.19	0.568	0.55	0.59
Y (XRF)	18	7	- -	36		
Zr	nd	460	422.60	270	289.70	190.90
Zr (XRF)	39	415	- -	239	- -	- -
Nb (XRF)	6	9	- -	6	- -	- -
Hf	nd	10.40	10.58	5.42	5.54	4.53
Ta	nd	0.939	0.95	0.65	0.67	0.43
Th	nd	7.08	7.23	2.00	2.00	6.95
U	nd	2.30	2.47	0.62	0.71	2.36
Co	nd	1.02	1.05	70.30	68.80	17.94
Cr	nd	7.80	8.42	77.10	76.01	12.56
Ni	nd		nd	- -	nd	nd
Sc	nd	15.10	14.81	40.20	39.06	21.72
Zn	nd	129	114.90	176	149.80	72.28
As	- -	- -	4.15	- -	9.37	3.79
Sb	nd	0.56	0.52	0.43	0.50	0.37

Table 9. *Major oxide and trace-element composition of Late and Middle Jurassic ultramafic-mafic complexes from map unit Juu from the Nulato quadrangle, west-central Alaska*

[Major elements in weight percent; trace elements in parts per million. All major oxides except FeO, CO_2, H_2O+, and H_2O- by X-ray fluorescence following methods of Taggart and others (1990). FeO by titration following method of Papp and others (1990). FeO values in italics calculated assuming $Fe_2O_3/FeO = 0.3$. CO_2 and H_2O by methods of Norton and Papp (1990). Trace elements by instrumental neutron activation analysis (INAA). LOI, loss on ignition. Methods described in Baedecker (1987). nd, not accurately determined (error greater than 15%); - -, not analyzed. USGS analyses done in Reston, Va., and Lakewood, Colo.]

Sample No.	82Pa4	74Pa127c	74Pa180b	79Pa552a	74Pa127a	79Pa521a	79Pa521b	79Pa525a	79Pa141b
Rock type	Diorite	Gabbro	Gabbro pegmatite	Gabbro	Amphibolite	Amphibolite	Amphibolite	Amphibolite	Amphibolite
Fig. 5 No.	24	25	26	27	28	29	30	31	32
Latitude	64°08.3'	64°12.0'	64°00.0'	64°00.0'	64°12.0'	64°18.4'	64°18.4'	64°12.0'	64°18.4'
Longitude	158°25.4'	156°30.6'	158°16.5'	158°16.5'	156°30.6'	156°23.3'	156°23.3'	156°30.6'	156°23.3'
SiO_2	61.1	49.2	49.6	49.8	49.5	48.4	48.3	50.7	44.4
Al_2O_3	17.4	16.3	16.0	16.1	16.0	17.7	20.1	15.7	17.4
Fe_2O_3	2.36	2.02	2.07	2.09	2.15	1.97	1.72	1.30	2.90
FeO	1.88	*6.95*	*7.13*	*7.21*	*7.43*	*6.79*	*5.92*	*4.49*	*10.00*
MgO	2.04	7.00	6.18	6.07	7.54	7.40	6.11	8.62	6.27
CaO	4.81	10.30	10.20	10.00	11.10	12.50	11.60	12.30	12.70
Na_2O	5.92	3.17	3.47	3.58	2.33	2.63	3.06	3.27	2.73
K_2O	0.68	0.83	0.53	0.55	0.12	0.17	0.25	0.13	0.10
TiO_2	0.8	1.05	1.11	1.12	0.99	0.78	0.50	0.43	1.43
P_2O_5	0.24	0.17	0.23	0.22	0.15	0.10	0.12	0.09	0.07
MnO	0.06	0.16	0.17	0.17	0.14	0.15	0.14	0.12	0.16
LOI	1.54	1.53	1.74	1.66	0.85	0.67	0.81	1.56	0.35
H_2O+	1.33	- -	- -	- -	- -	- -	- -	- -	- -
H_2O-	0.20	- -	- -	- -	- -	- -	- -	- -	- -
CO_2	0.06	- -	- -	- -	- -	- -	- -	- -	- -
Total	98.88	97.15	96.69	96.92	97.45	98.58	97.82	97.16	98.16
Rb	- -	11.93	9.49	9.36	nd	nd	nd	nd	nd
Sr	- -	530.10	1362.00	1621.00	199.30	560.70	840.30	nd	788.20
Ba	- -	310.00	391.40	455.00	nd	99.89	nd	nd	nd
La	- -	5.06	6.67	6.50	3.02	1.95	2.44	1.94	0.73
Ce	- -	12.30	15.09	15.13	8.16	5.01	5.22	5.14	nd
Nd	- -	8.26	10.24	11.34	7.01	nd	3.76	nd	nd
Sm	- -	2.92	3.565	3.47	2.51	1.42	1.32	1.46	1.10
Eu	- -	0.98	1.10	1.17	0.89	0.65	0.63	0.49	0.55
Tb	- -	0.57	0.66	0.66	0.57	0.29	0.21	0.35	0.19
Yb	- -	2.17	2.49	2.55	2.33	1.04	0.64	1.61	nd
Lu	- -	0.34	0.37	0.37	0.36	0.16	0.10	0.23	0.09
Hf	- -	1.91	2.13	2.13	1.41	0.64	0.33	1.00	nd
Ta	- -	0.19	0.21	0.22	0.17	nd	nd	nd	nd
Th	- -	0.63	0.59	0.68	nd	nd	nd	nd	nd
U	- -	nd	nd	0.23	nd	nd	nd	nd	nd
Co	- -	30.15	33.25	33.65	42.90	35.89	31.47	30.90	42.01
Cr	- -	163.50	107.70	90.56	113.90	261.20	137.50	486.10	21.11
Ni	- -	nd	nd	nd	nd	90.61	nd	157.10	nd
Sc	- -	38.19	36.29	34.99	40.80	33.89	27.91	29.02	42.24
Zn	- -	73.62	60.78	58.65	52.07	52.15	49.24	36.71	73.75
Au	- -	nd	nd	nd	nd	16.16	nd	nd	nd

Table 10. *Major oxide and trace-element composition of Triassic to Mississippian altered basalt, gabbro, and chert from map unit* $\overline{\mathrm{R}}$*Mb from the Nulato quadrangle, west-central Alaska*

[Major elements in weight percent; trace elements in parts per million. All major oxides except FeO, CO_2, H_2O+, and H_2O- by X-ray fluorescence following methods of Taggart and others (1990). FeO by titration following method of Papp and others (1990). CO_2 and H_2O by methods of Norton and Papp (1990). Trace elements by instrumental neutron activation analysis (INAA) unless otherwise noted in first column by following acronyms: XRF, energy-dispersive X-ray fluorescence; ICP, inductively coupled plasma-emission spectrometry. LOI, loss on ignition. Methods described in Baedecker (1987). nd, not accurately determined (error greater than 15%); - -, not analyzed. USGS analyses done in Lakewood, Colo. ADGGS samples previously published in Solie and others (1993c)]

Sample No.	82Pa1	82Pa2	82Pa242	82Pa248	82Pa249	82Pa253	ADGGS2412	ADGGS2461
Analyses by	USGS	USGS	USGS	USGS	USGS	USGS	ADGGS	ADGGS
Rock type	Diabase	Diabase	Diabase	Diabase	Diabase	Diabase	Basalt	Basalt
Fig. 5 No.	32	33	34	35	36	37	38	39
Latitude	64°13.9'	64°12.3'	64°07.4'	64°24.0'	64°15.2'	64°25.9'	64°21.7'	64°22.2'
Longitude	158°23.5'	158°24.3'	156°31.8'	156°25.6'	156°41.8'	156°50.4'	157°13.6'	157°14.6'
SiO_2	47.8	48.6	48.0	50.1	47.6	46.5	48.2	46.5
Al_2O_3	12.8	16.7	15.1	13.9	12.4	14.8	13.4	12.0
Fe_2O_3	3.29	3.10	1.69	2.65	2.52	2.48	2.46	2.29
FeO	10.10	5.16	8.93	8.33	8.09	8.94	7.60	6.10
MgO	6.93	6.56	6.80	6.47	7.23	7.04	8.46	11.80
CaO	8.89	9.84	10.40	7.76	10.30	11.10	11.50	14.70
Na_2O	4.09	2.75	2.28	2.62	2.68	2.38	2.11	1.26
K_2O	0.02	1.30	0.77	0.55	1.88	0.10	0.42	0.20
TiO_2	1.51	0.98	1.80	1.83	3.26	1.68	1.27	0.60
P_2O_5	0.16	0.23	0.15	0.19	0.40	0.14	0.13	0.05
MnO	0.24	0.13	0.17	0.26	0.15	0.15	0.17	0.14
LOI	3.17	4.15	2.9	4.22	2.11	3.77	3.77	3.77
H_2O+	3.31	3.05	3.18	4.34	2.51	4.41	- -	- -
H_2O-	0.25	0.50	0.30	0.40	0.19	0.20	- -	- -
CO_2	0.40	0.90	<.01	0.05	<.01	0.01	- -	- -
Total	99.79	99.80	99.57	99.45	99.21	99.93	99.49	99.41
Rb (XRF)	2	22	17	10	41	5	26	13
Sr (XRF)	61	600	298	127	577	129	233	165
Ba (XRF)	60	231	570	120	554	233	399	202
La	4.80	7.43	8.55	14.90	26.70	5.10	- -	- -
Ce	11.1	17.7	21.4	34.8	67.2	15.4	- -	- -
Nd	7.90	12.0	13.2	21.6	34.3	10.7	- -	- -
Sm	2.77	3.37	3.97	5.82	8.12	3.10	- -	- -
Eu	0.996	1.09	1.39	1.87	2.55	1.14	- -	- -
Gd	3.75	3.46	4.43	6.20	7.85	4.20	- -	- -
Tb	0.695	0.536	0.644	0.860	1.09	0.74	- -	- -
Dy	4.65	3.49	4.00	5.60	6.40	5.30	- -	- -
Tm	0.483	0.309	0.303	0.400	0.361	0.46	- -	- -
Yb	3.25	1.92	1.78	2.52	2.14	2.94	- -	- -
Lu	0.514	0.296	0.262	0.350	0.290	0.456	- -	- -
Y (XRF)	31	21	21	28	27	29	22	15
Zr (XRF)	81	73	108	137	220	101	73	34
Nb (XRF)	10	6	12	16	34	11	11	18
Co (ICP)	55	36	44	40	44	50	- -	- -
Cr (XRF)	- -	- -	- -	- -	- -	- -	235	707
Ni (ICP)	74	61	92	34	118	87	- -	- -
Sc (ICP)	64	38	43	38	34	50	- -	- -